



Megathrust friction in the 2010 Maule earthquake area in relation to forearc morphology and mechanical stability, and to earthquake rupture dynamics

Nadaya Cubas

J.P. Avouac, N. Lapusta

Coll. : Y. Leroy, P. Souloumiac

Megathrust friction in the 2010 Maule earthquake area

1. Introduction

2. From the Critical Taper Theory

3. From Limit Analysis

4. From Dynamic Simulation of EQ cycle

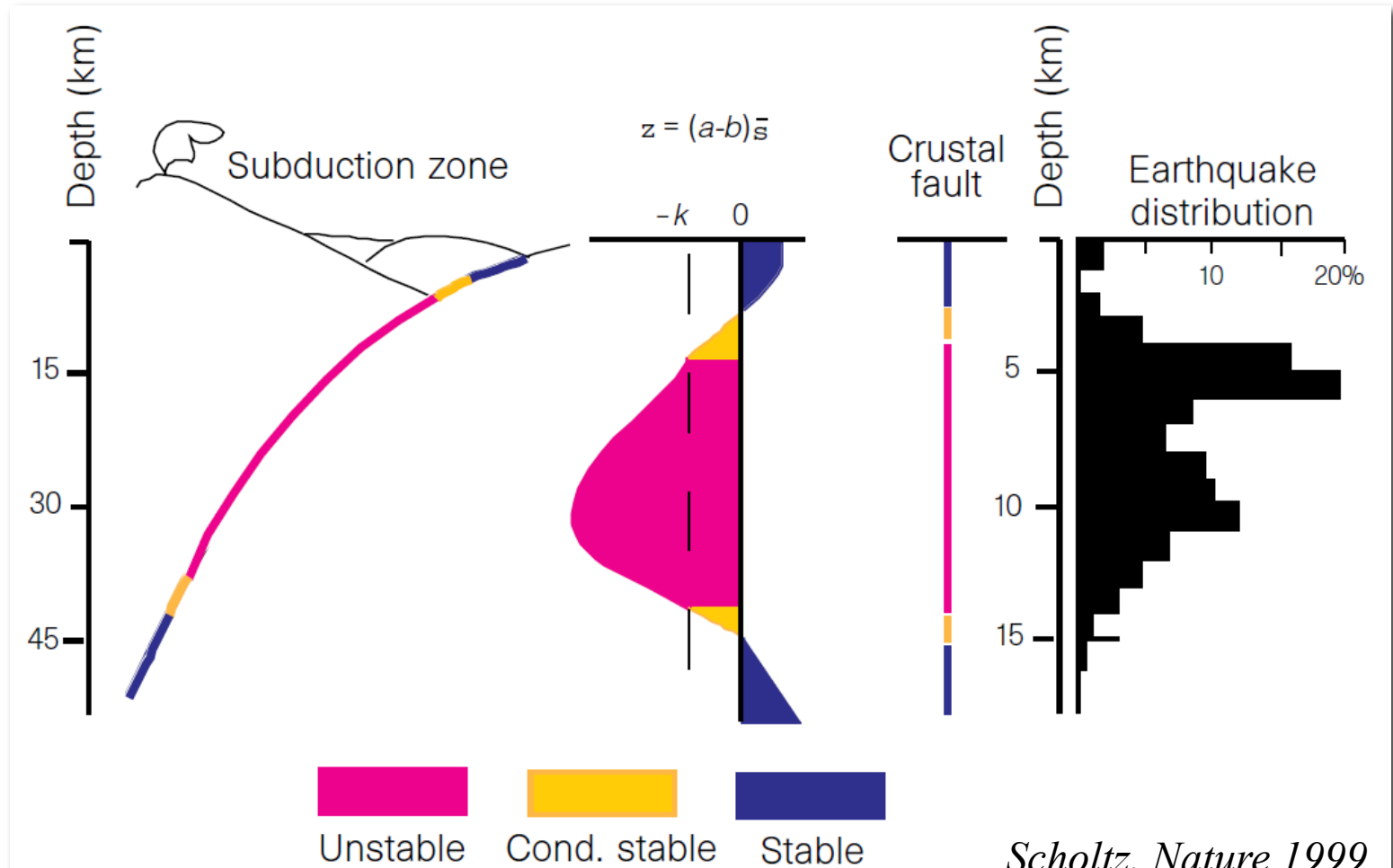
1. Introduction

Spatial variations of frictional properties: Rate-and-state laws

$$\mu_{SS} = \tau/\sigma = \mu_* + (a-b) \ln(V/V_*)$$

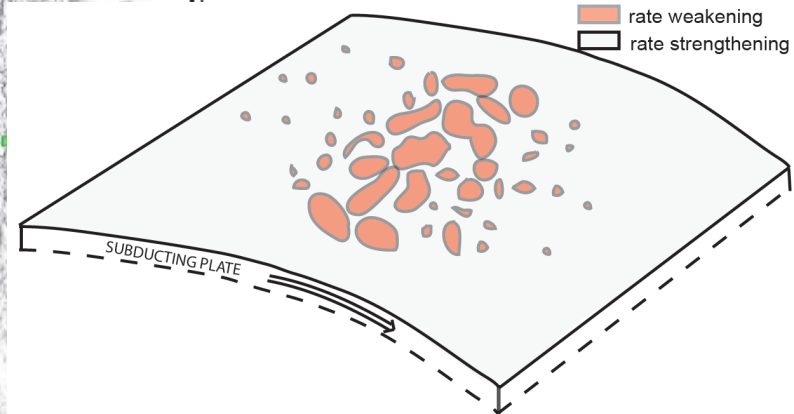
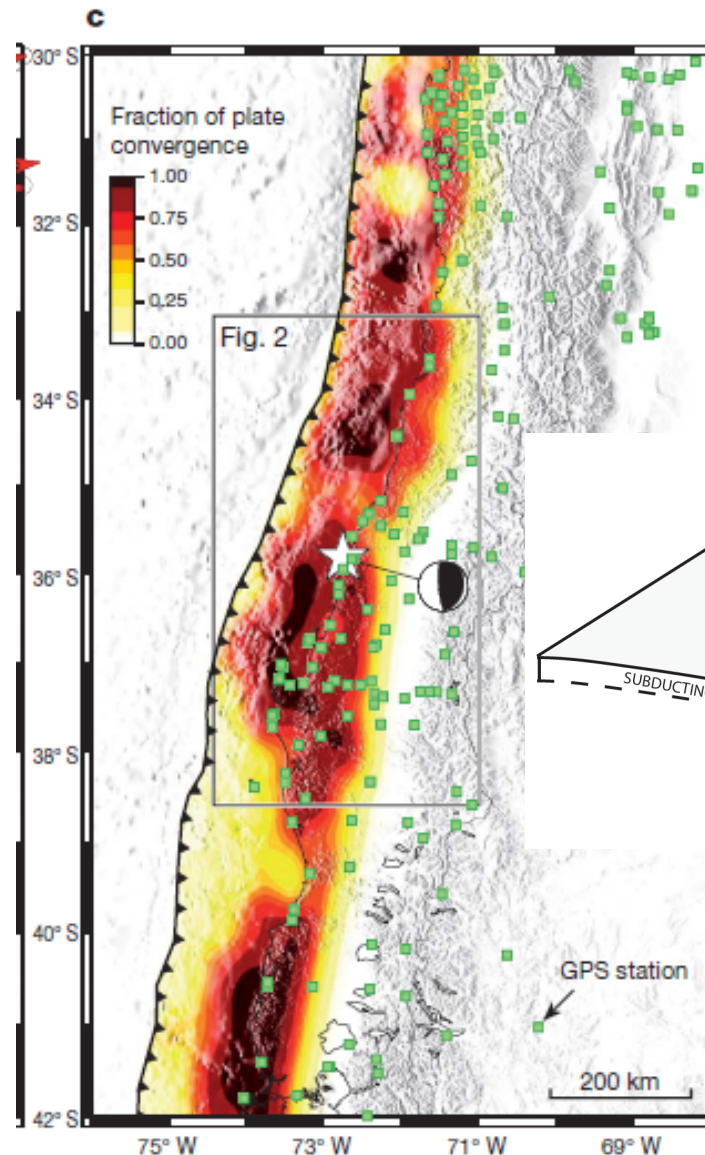
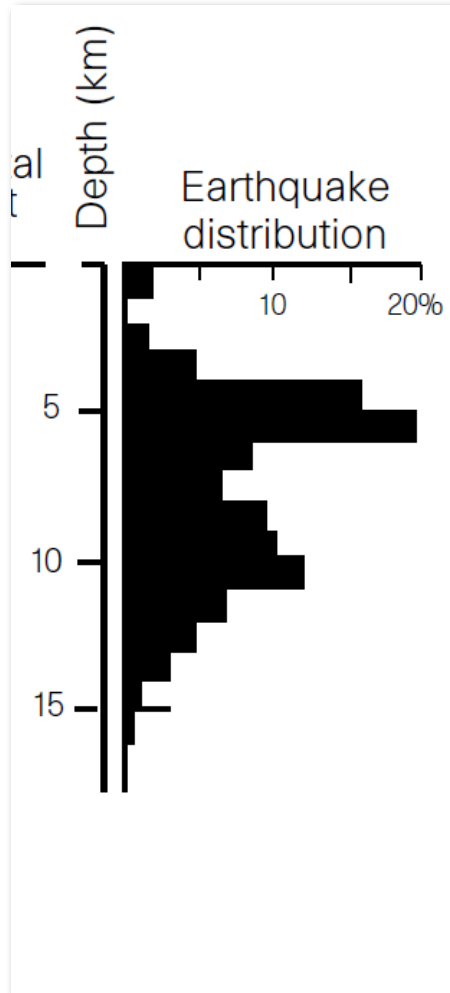
$(a-b) > 0$ rate-strengthening : $\mu_s < \mu_d$

$(a-b) < 0$ rate-weakening : $\mu_s > \mu_d$



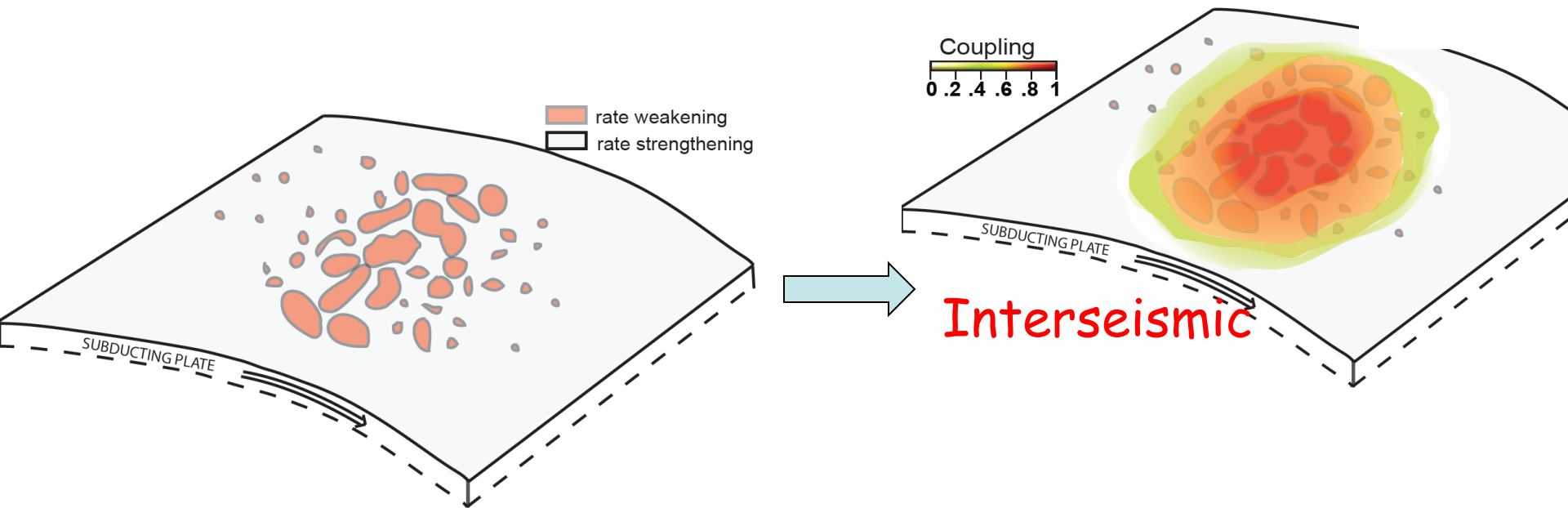
1. Introduction

Spatial variations of frictional properties: Interfingering patches

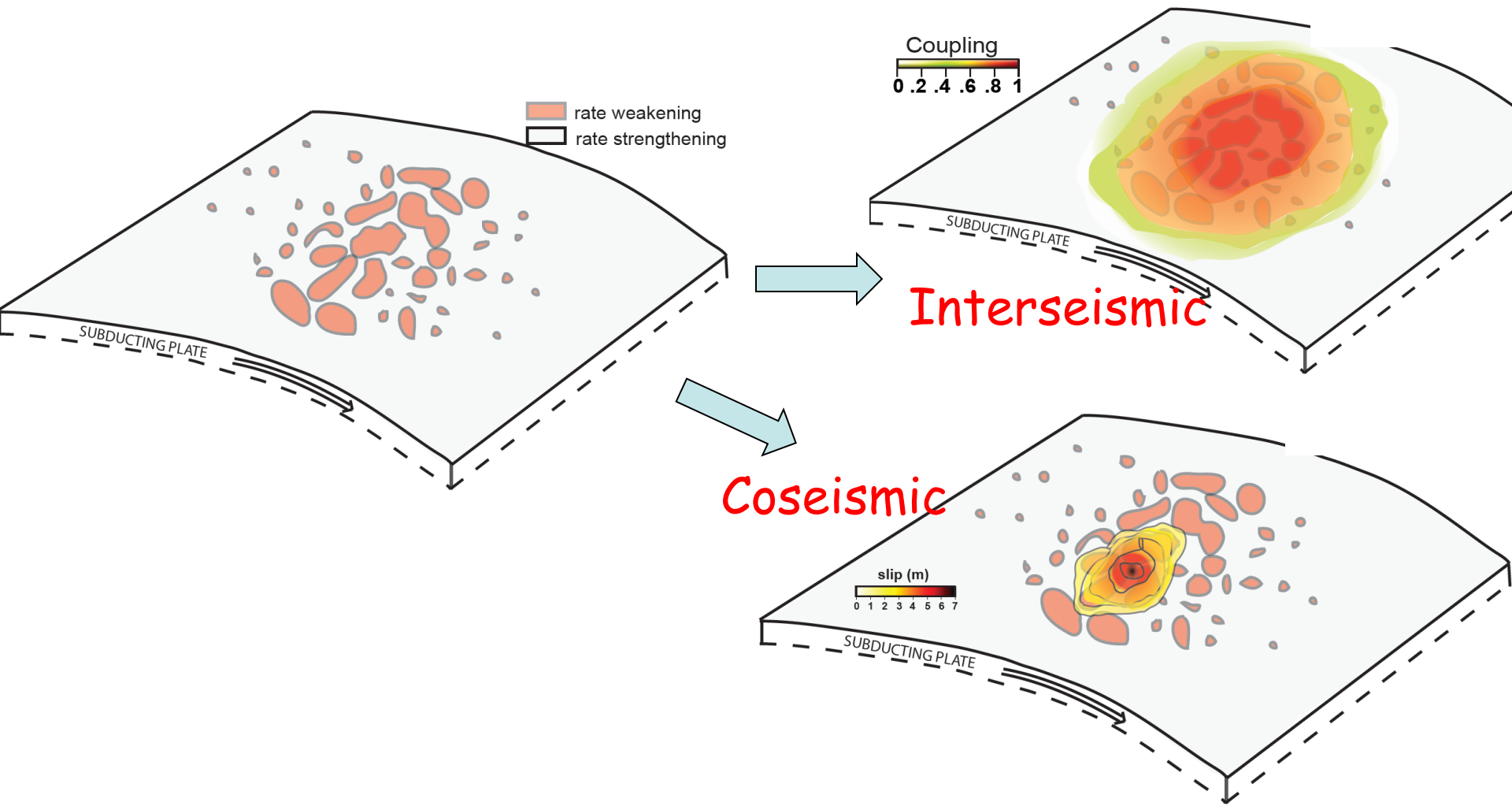


(Moreno *et al.*, *Nature*, 2010)

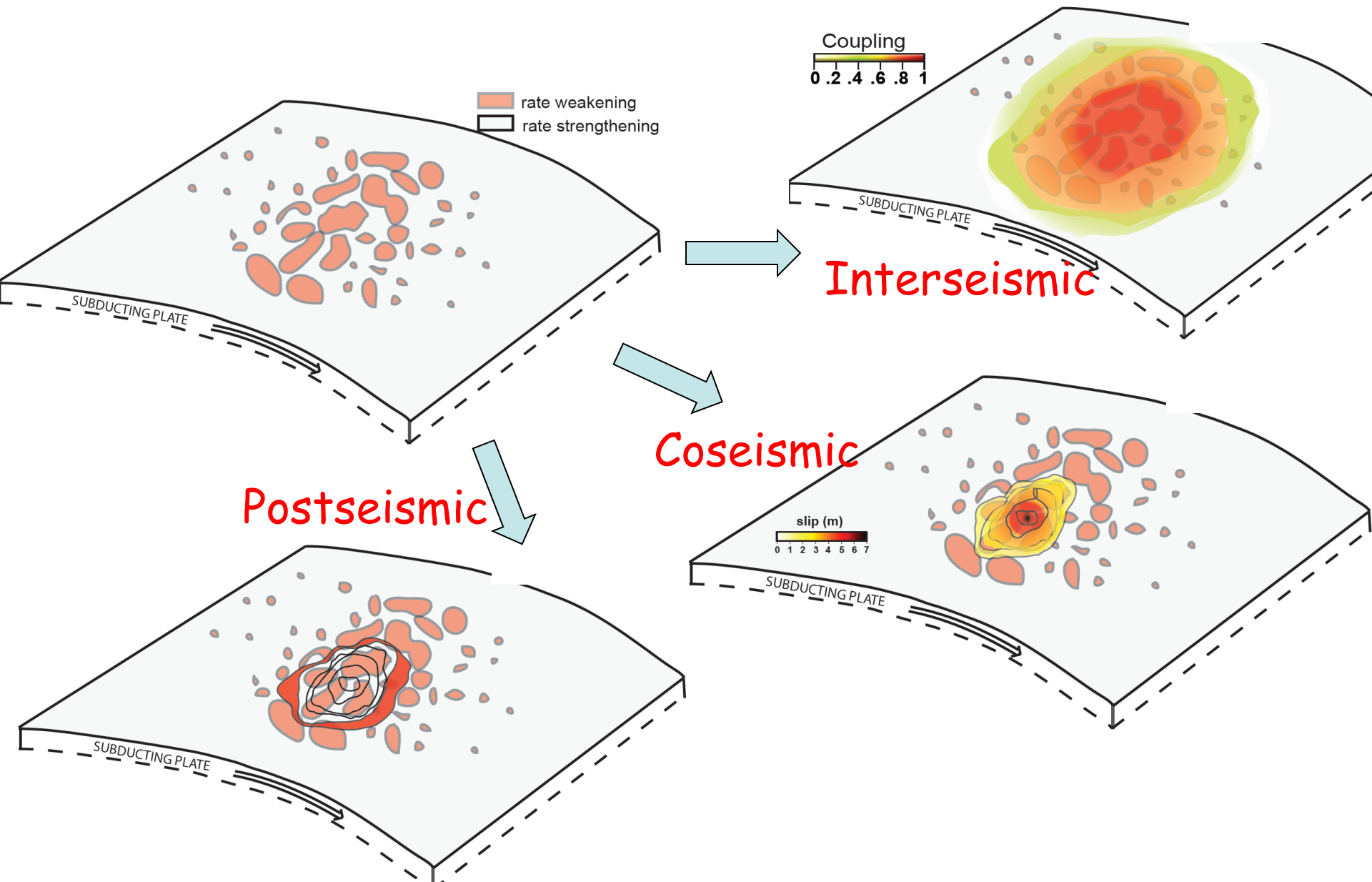
1. Introduction



1. Introduction



1. Introduction



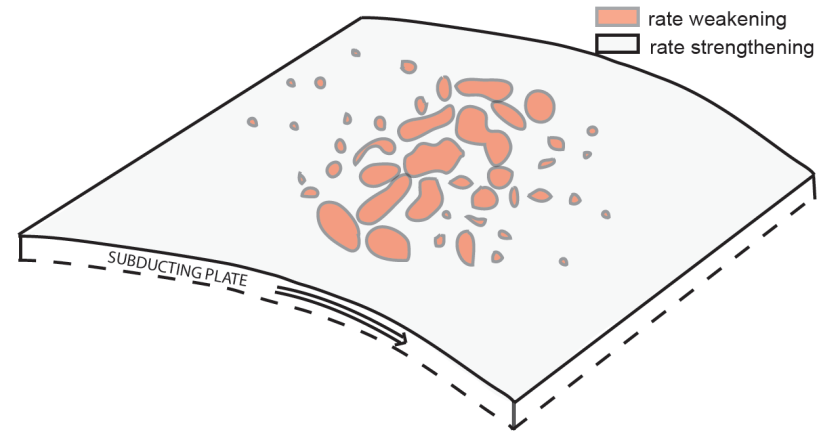
1. Introduction

Objective :

Spatial variations of fault friction: observations and implication for fault dynamics

develop realistic (predictive?) dynamic models of the seismic cycle.

$$\mu_{ss} = \tau/\sigma = \mu_* + (a-b) \ln(V/V_*)$$



Some outstanding questions:

- What are the frictional properties of faults?
- How do these properties vary in space and time?
- How do they influence individual earthquakes or the long-term seismic behavior of a fault?

1. Introduction

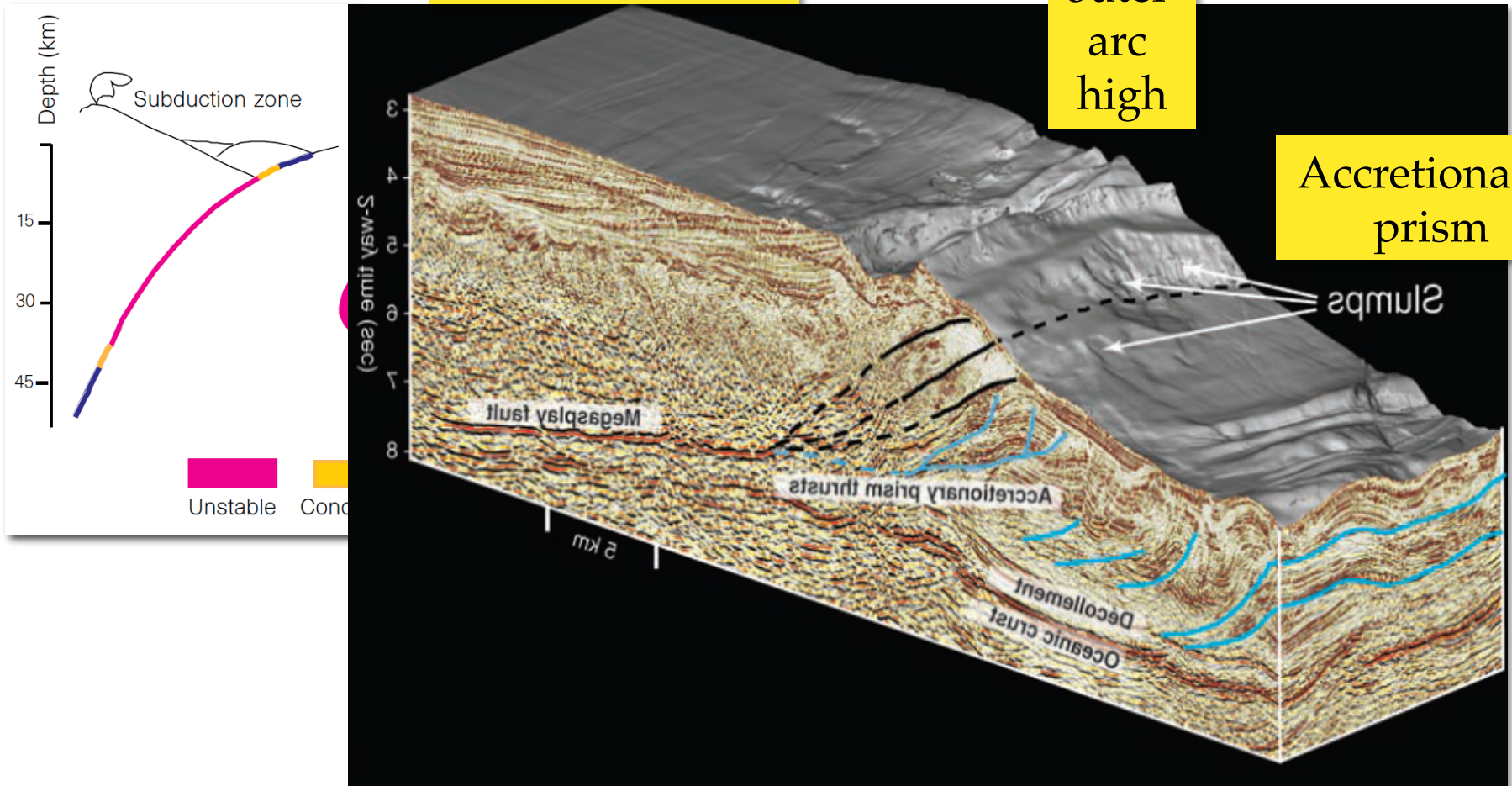
Morpho-tectonic segmentation of forearc

Nankai:

Forearc basin or
deep sea-terrace

outer
arc
high

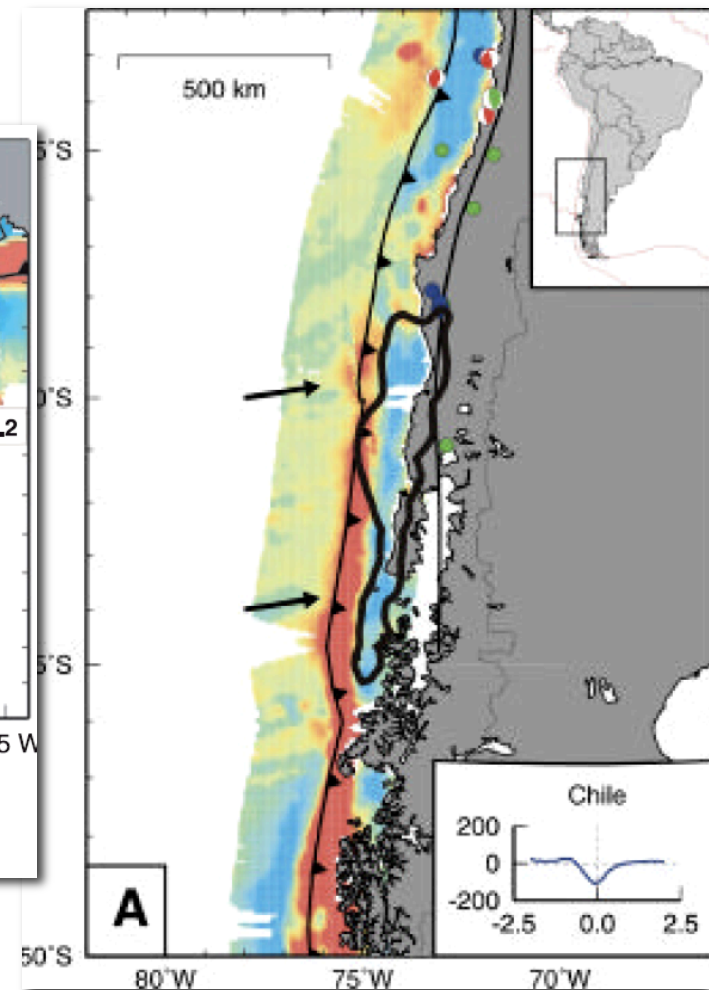
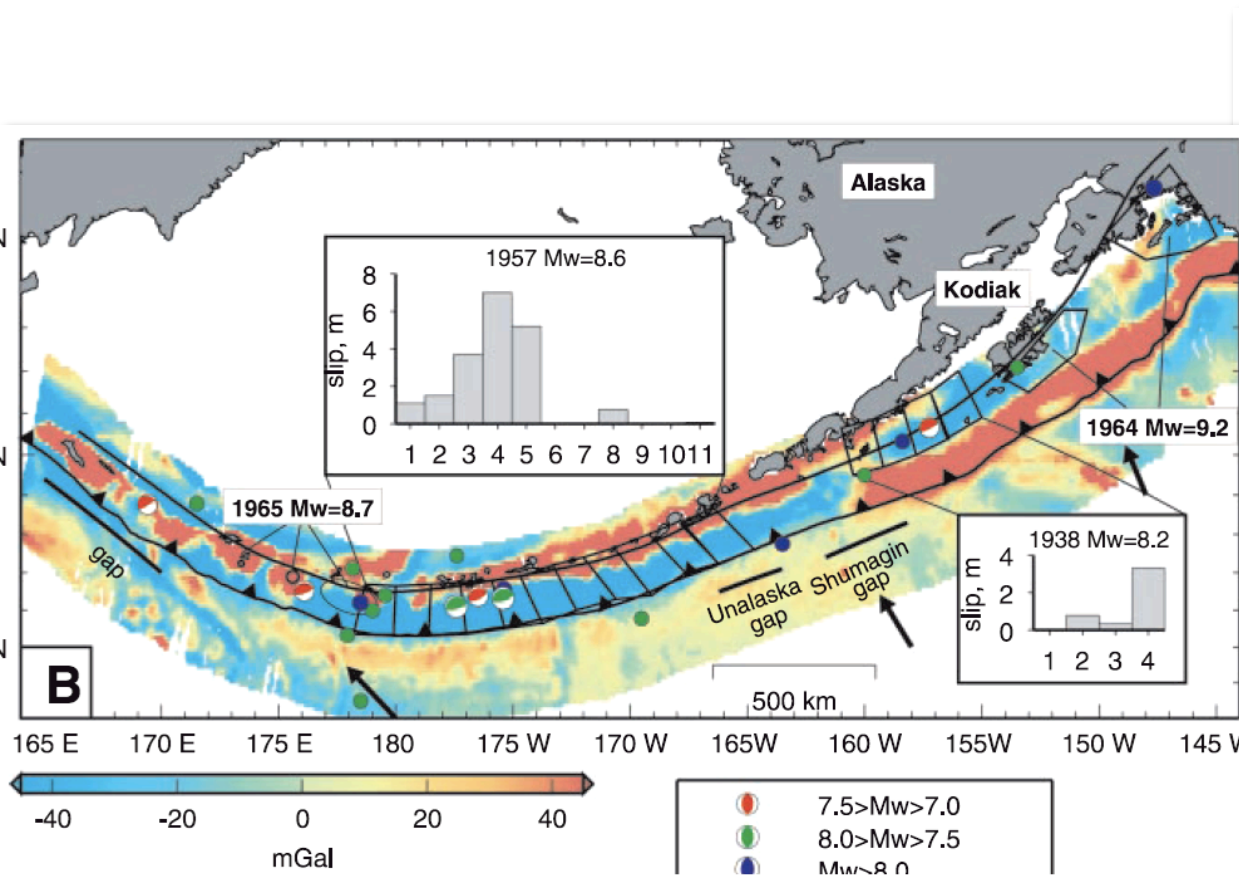
Accretionary
prism



1. Introduction

Spatial variations of frictional properties: Related to the forearc morphology

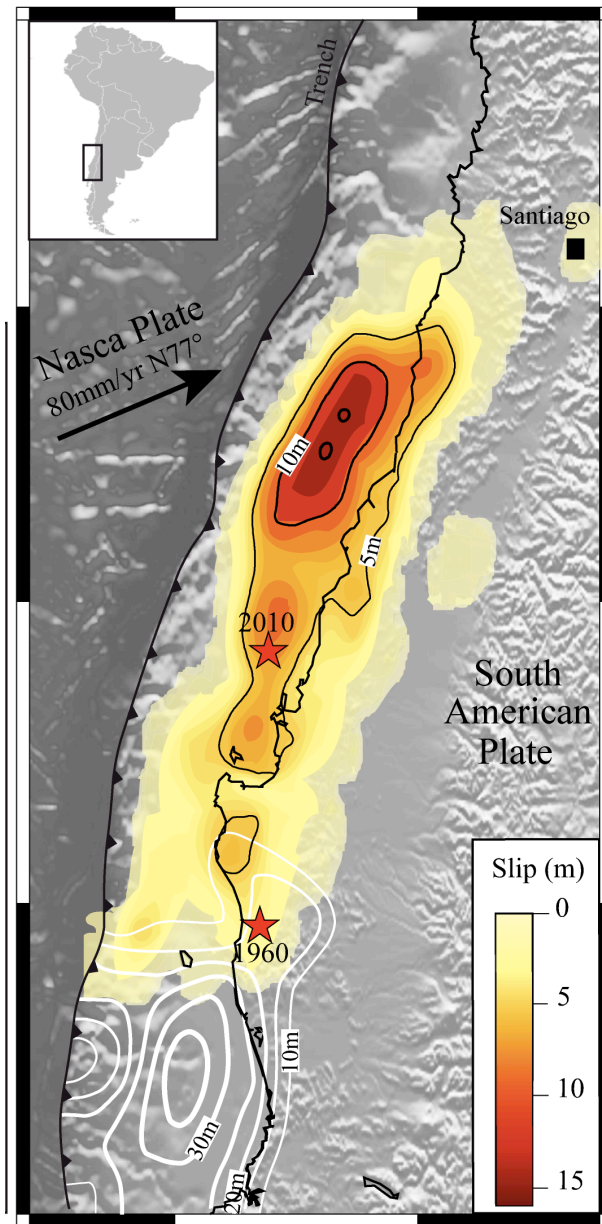
Song & Simons, Science 2003



Correlation between seismic asperities of great earthquakes and trench-parallel gravity anomaly

1. Introduction

Maule 2010, Mw 8.8



Coseismic slip from Lin et al., in prep. -74° -72°

Megathrust friction in the 2010 Maule earthquake area

1. Introduction

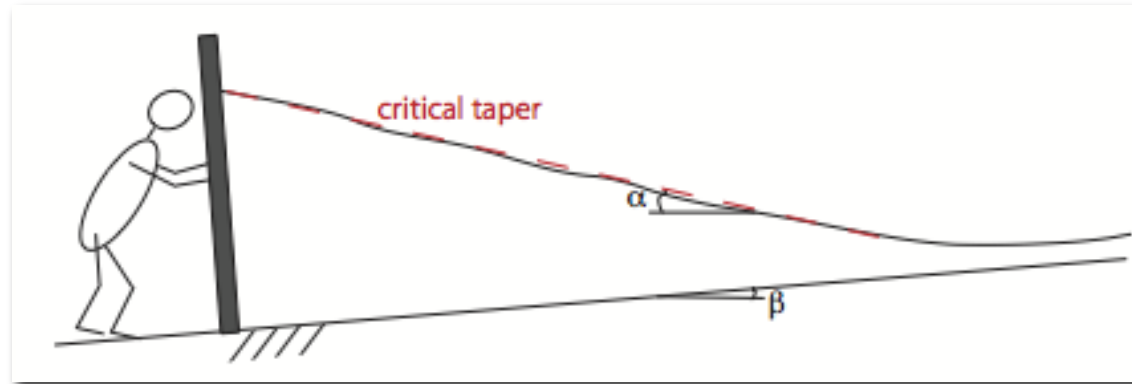
2. From the Critical Taper Theory

3. From Limit Analysis

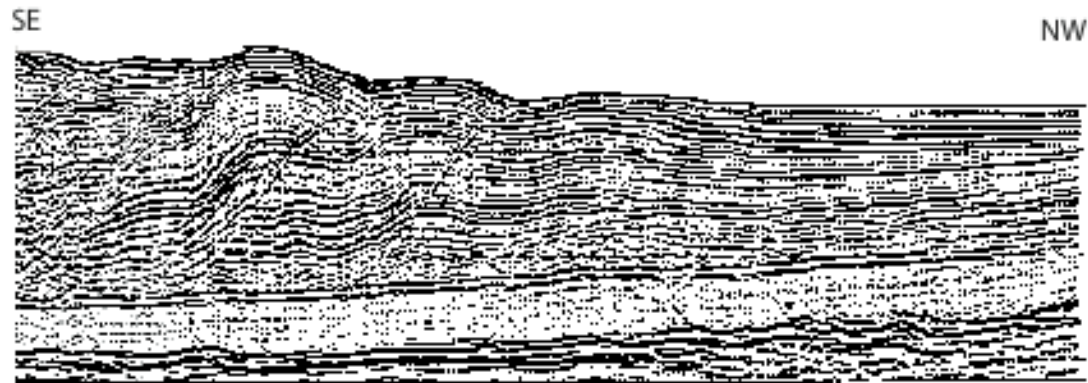
4. From Dynamic Simulation of EQ cycle

2. Critical Taper

Analogue of sand wedges pushed by bulldozer:
(Davis et al., JGR 1983)



Nankai wedge :

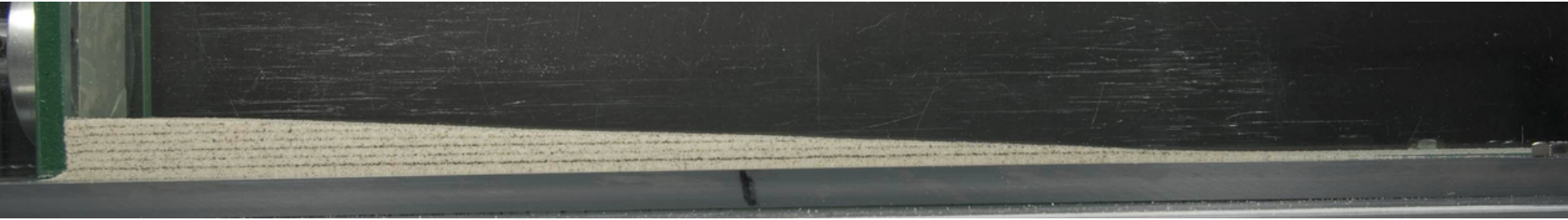


Morgan and Karig, 1994

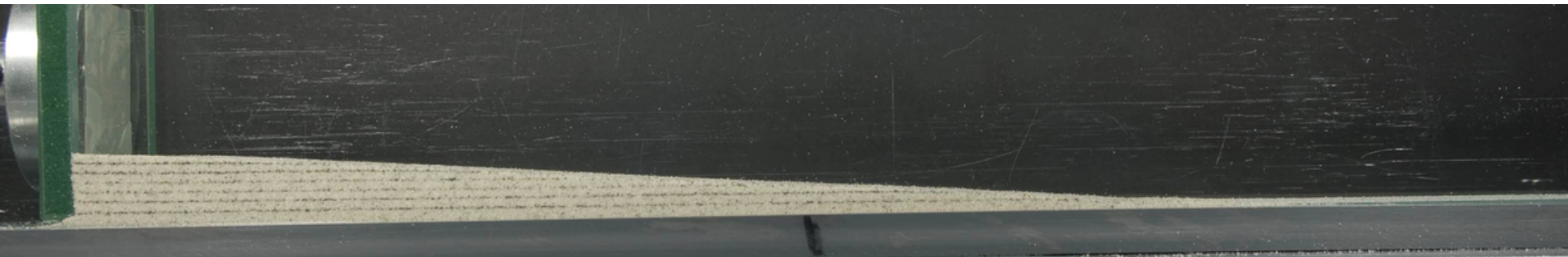
1km

2. Critical Taper

Unstable / Sub-critical :



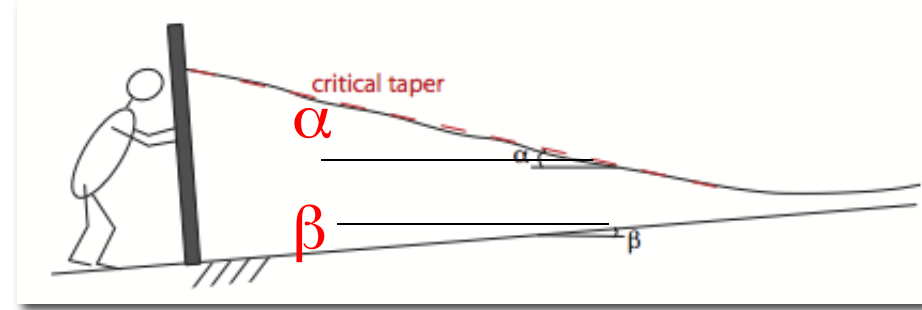
Stable / over-critical :



Courtesy of Souloumiac P.

2. Critical Taper

Theory (Dahlen, JGR 1984):



$$\alpha_c = \frac{1}{2} \arcsin\left(\frac{\sin\phi'_b}{\sin\phi_b}\right) - \frac{1}{2}\phi'_b - \frac{1}{2} \arcsin\left(\frac{\alpha'}{\sin\phi}\right) - \frac{1}{2}\alpha' - \beta$$

Critical topographic slope

Basal friction

Internal friction

Decollement dip

$$\mu = \tan\phi$$

$$\mu_b = \tan\phi_b$$

$$\mu'_b = \mu_b \frac{(1-\lambda_b)}{(1-\lambda)}$$

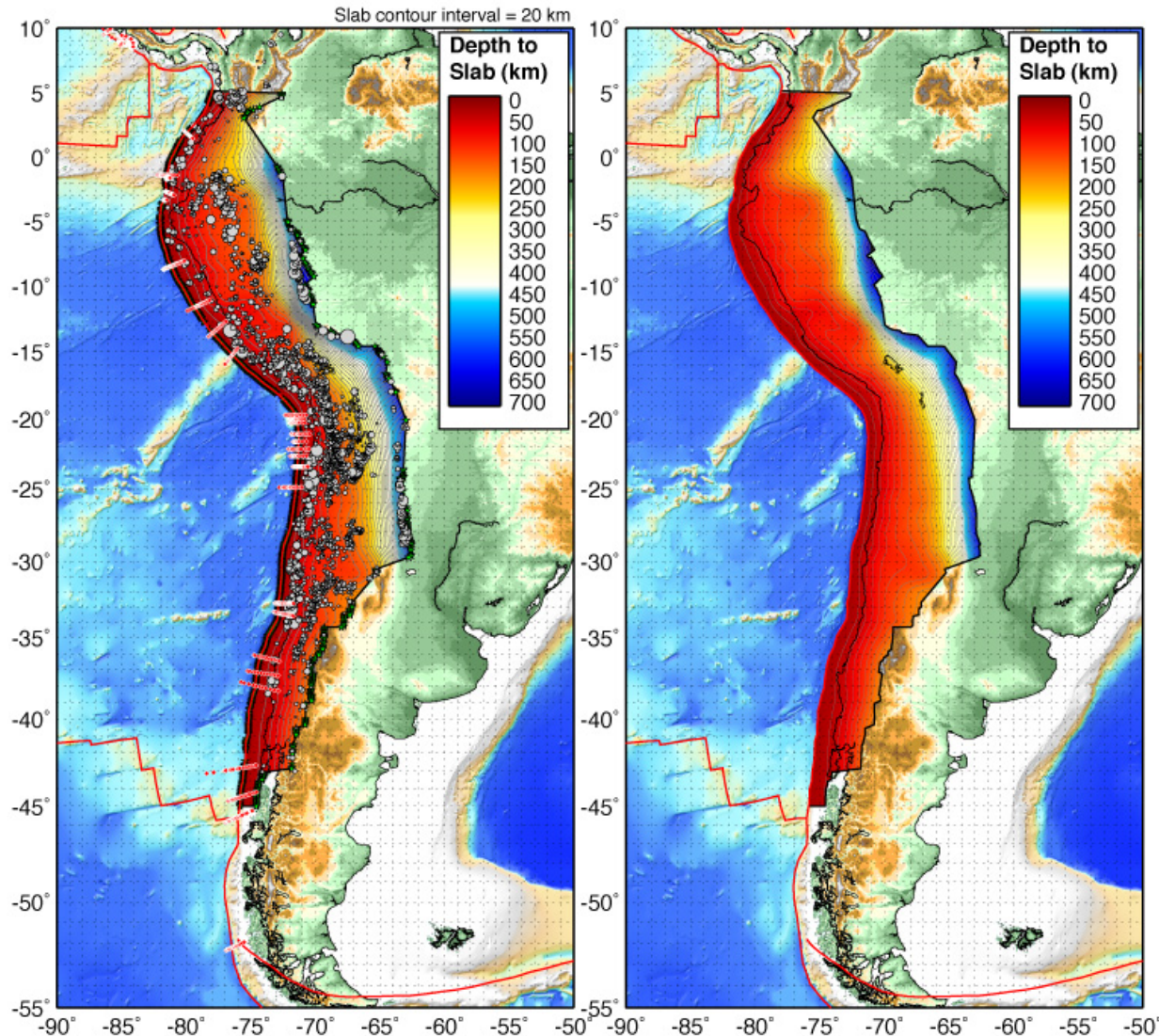
$$\mu' = \mu(1-\lambda)$$

$$\alpha' = \arctan\left(\frac{1-\rho_w/\rho}{1-\lambda} \tan\alpha\right)$$

$$\Lambda \sim \mathbf{p}_f / \sigma_z$$

2. Critical Taper

Covariation α/β : Slab morphology (*Hayes & Wald, GJI 2009*)

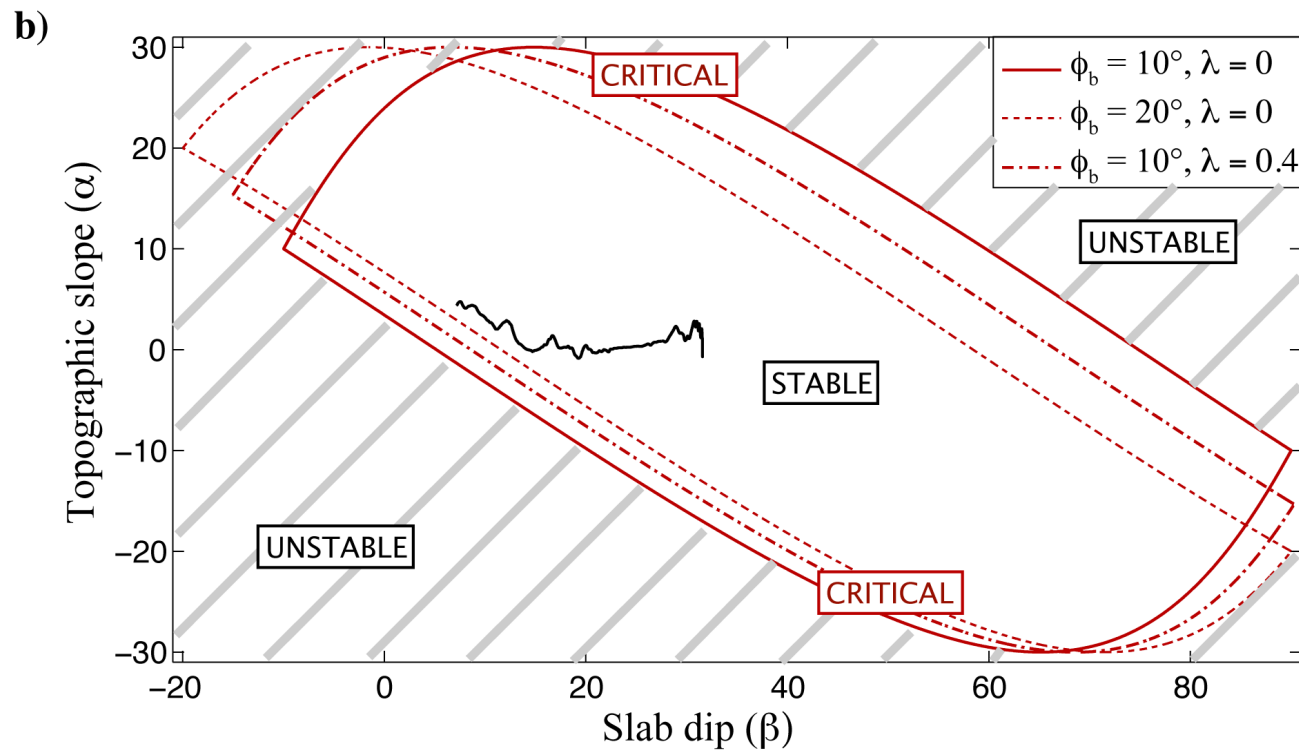
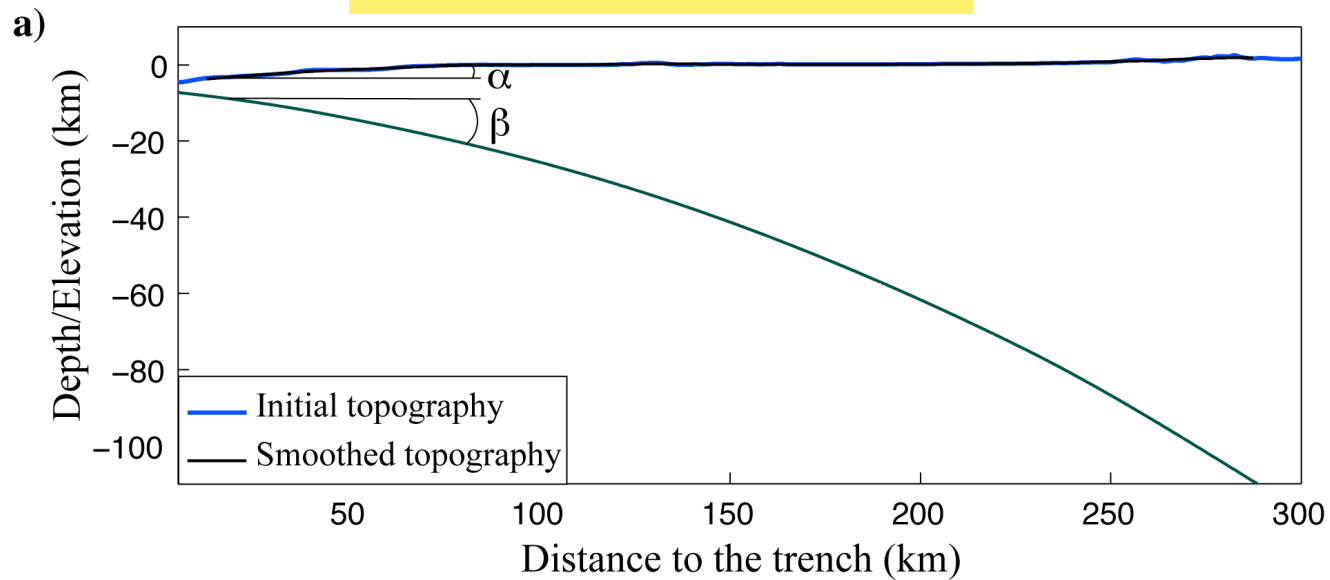


Slab 1.0 : *Hayes & Wald, GJI 2009*, construct probability density functions to solve for the 'most-likely' fault plane, by incorporating data from historic earthquake catalogues (gCMT, NEIC PDE and the global relocation catalogue of Engdahl et al. (1998)), locations of trench breaks on the seafloor (from the plate boundary files of Tarr et al. 2009) and any 'new' event location (both NEIC hypocentre and gCMT centroid)

Topography : ETOPO1, *Amante and Eakins, 2009*.

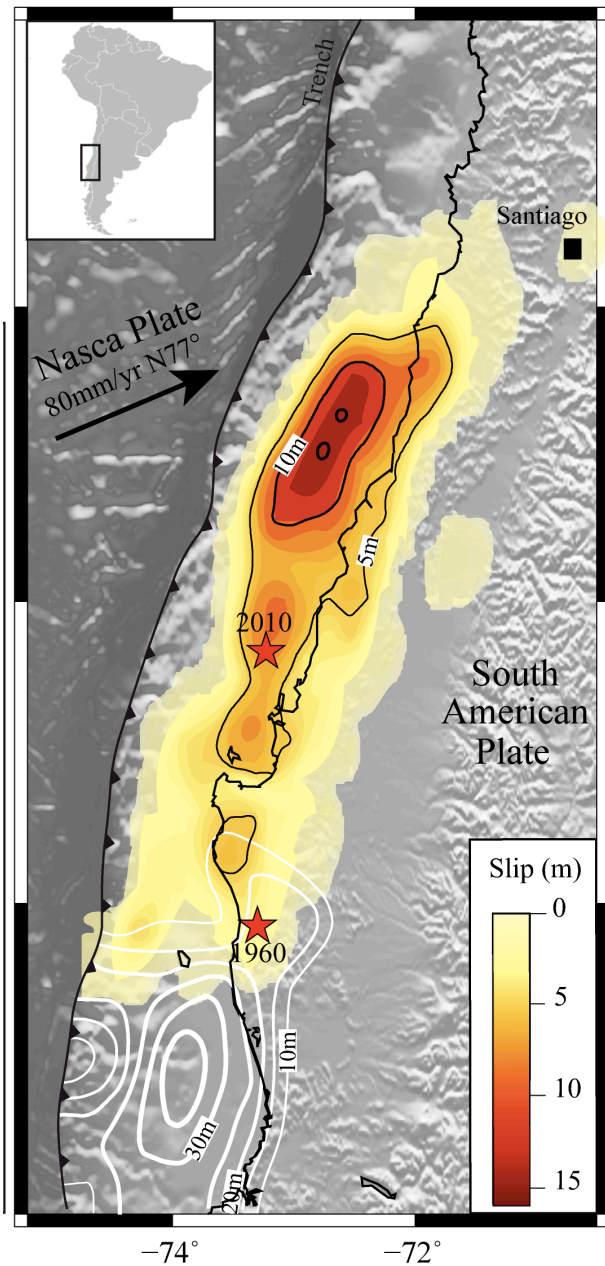
2. Critical Taper

Forearc: At critical state?

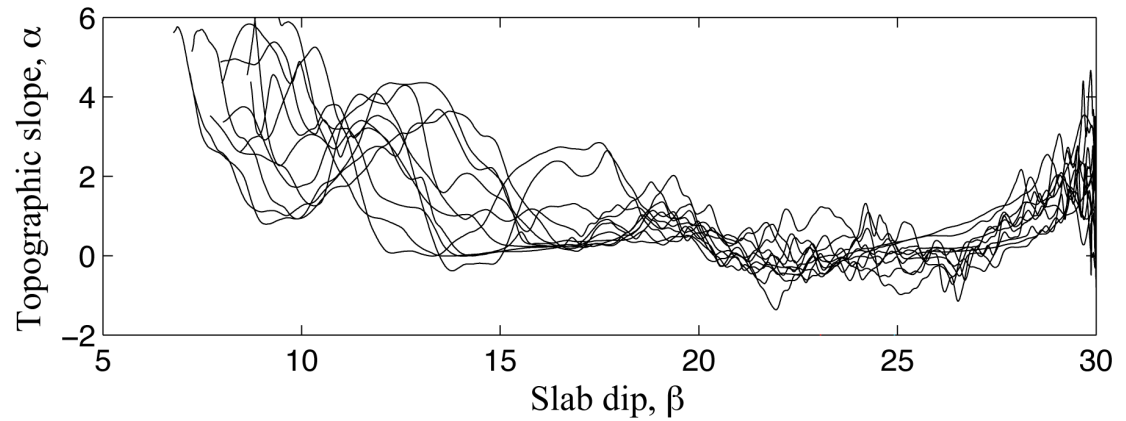


2. Critical Taper

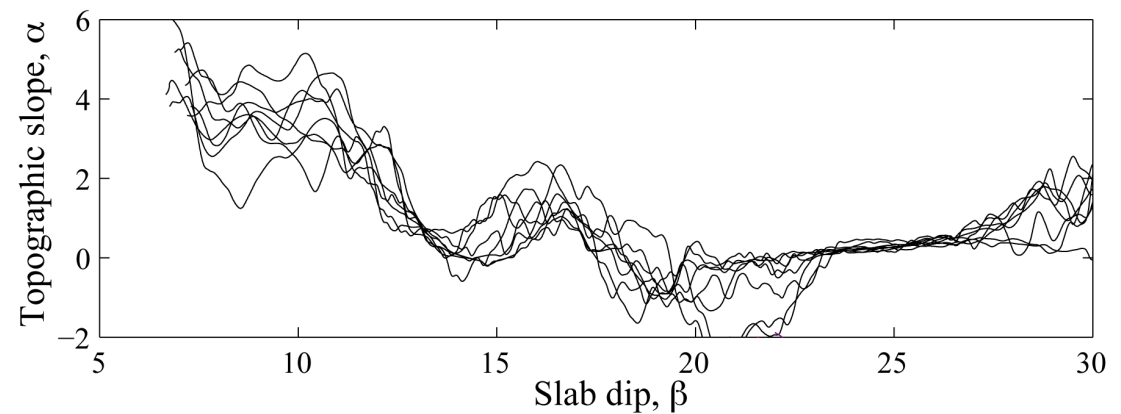
Forearc: At critical state?



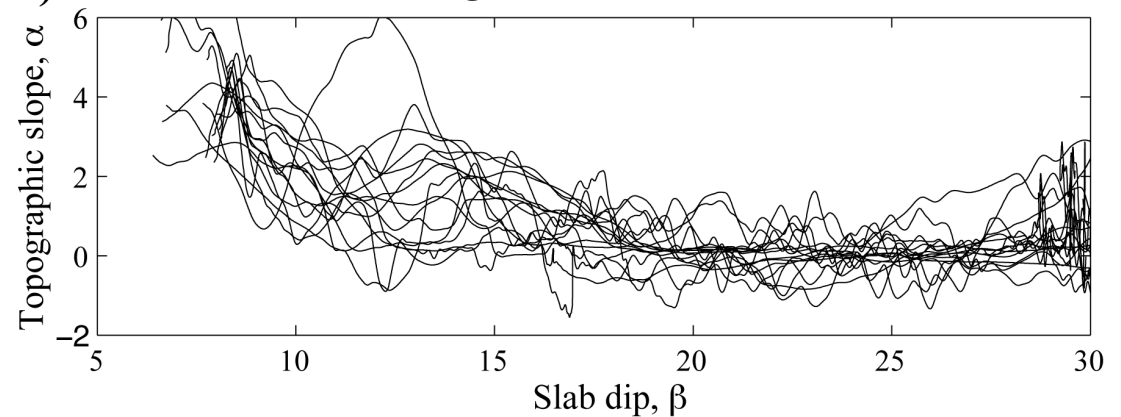
a) Maule segment



b) Arauco Peninsula segment

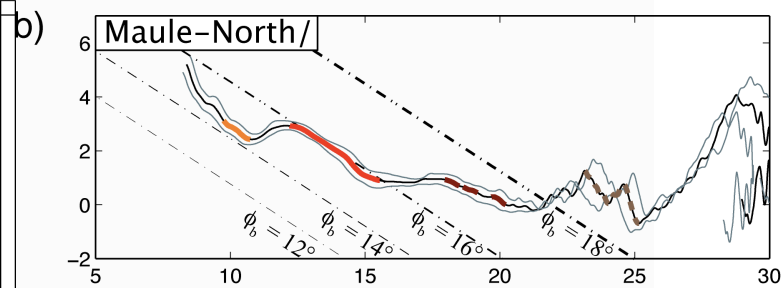
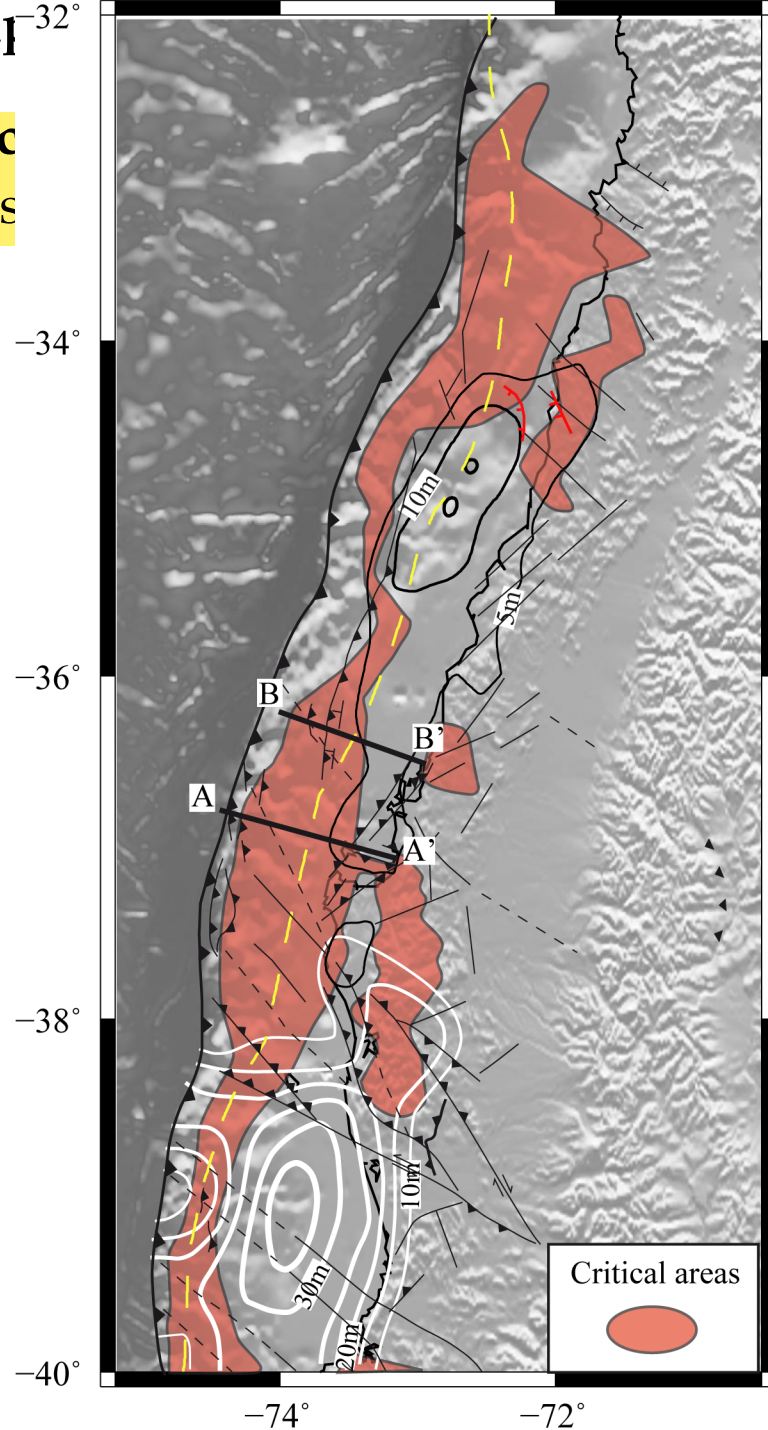


c) North Valdivia segment



2. Critical Taps^{32°}

Forearc
At critical s



Arauco peninsula:

Uplift rate = 1.8 ± 0.4 mm/a over the past 50 ka (Melnick *et al.*, 2006) and of 2.3 ± 0.2 mm/a over the past 3 ka (Bookhagen *et al.*, 2006)

Nahuelbuta range:

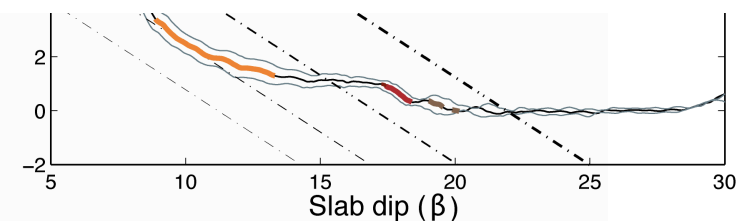
twice the relief of coastal cordillera, with an increase of uplift rate since 4Ma >0.2 mm/a (Glodny *et al.*, 2008)

Tolten:

no evidence

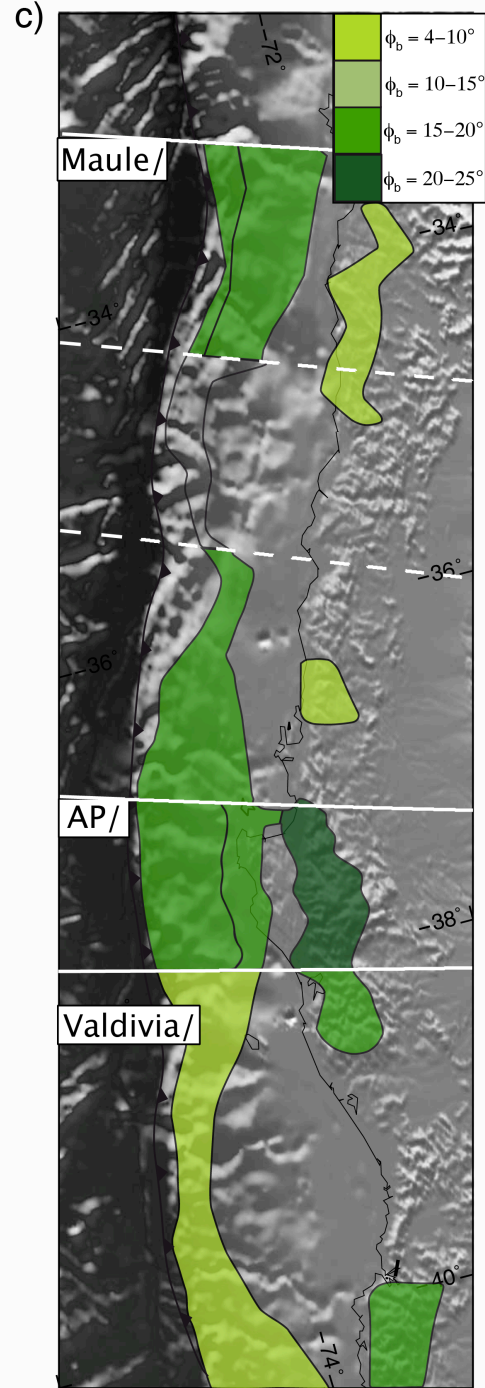
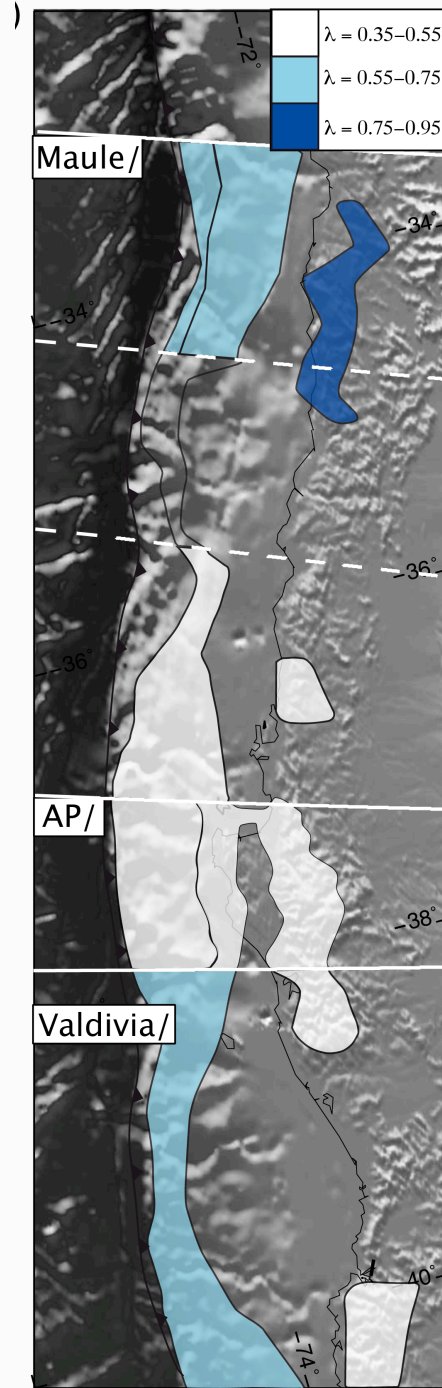
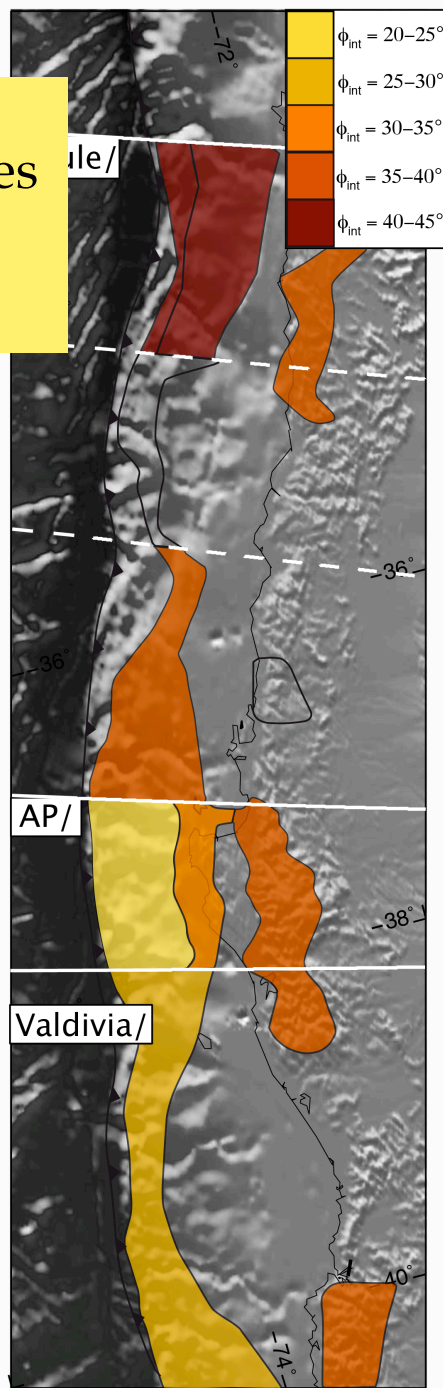
Bueno segment:

quaternary uplift (Rehak *et al.*, *Geom.* 2008)



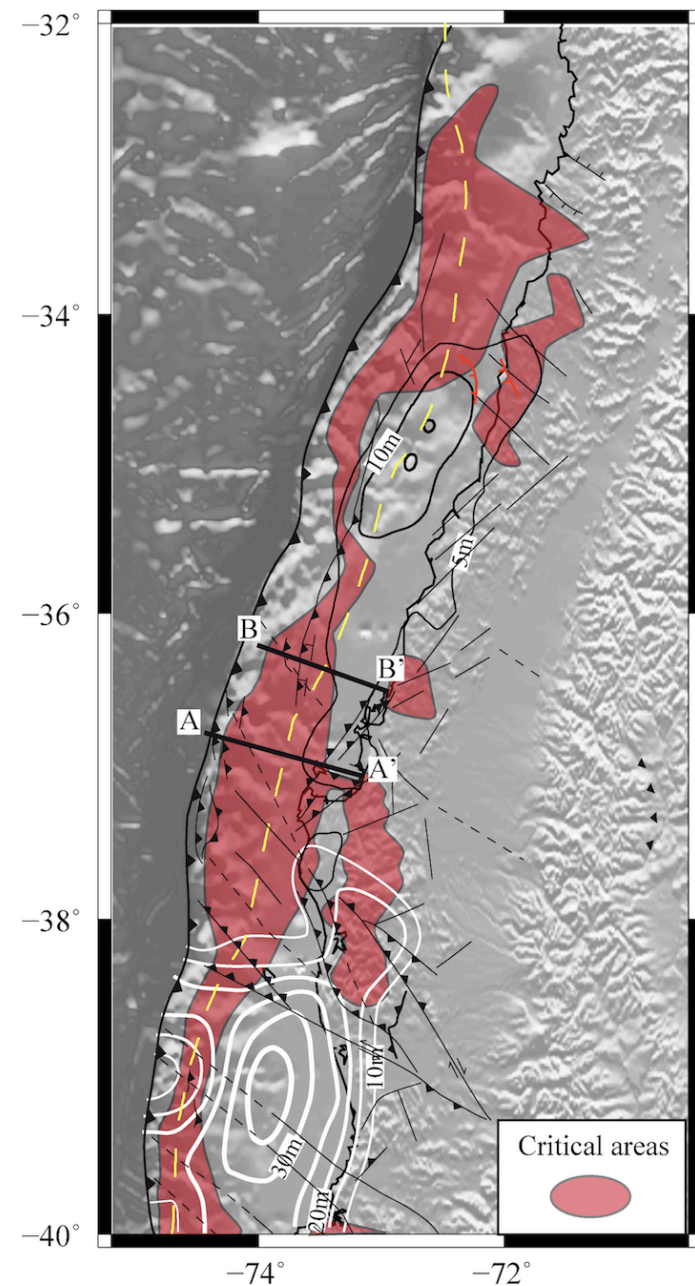
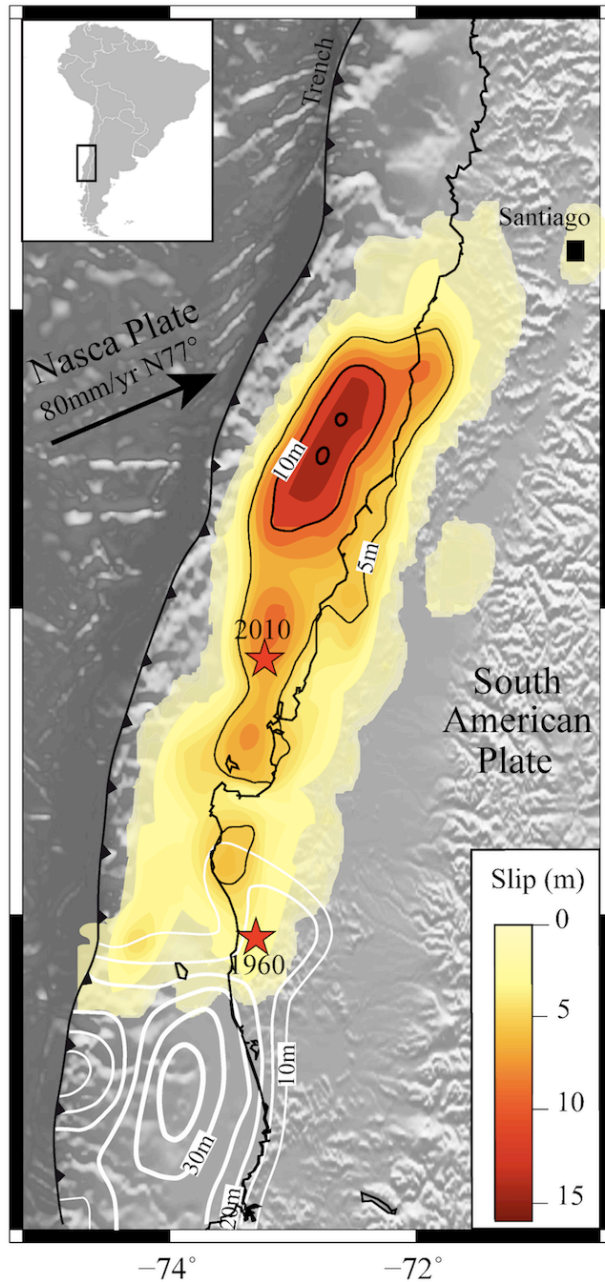
2. Critical Taper a)

Forearc:
Frictional properties
obtained from
inversion



2. Critical Taper

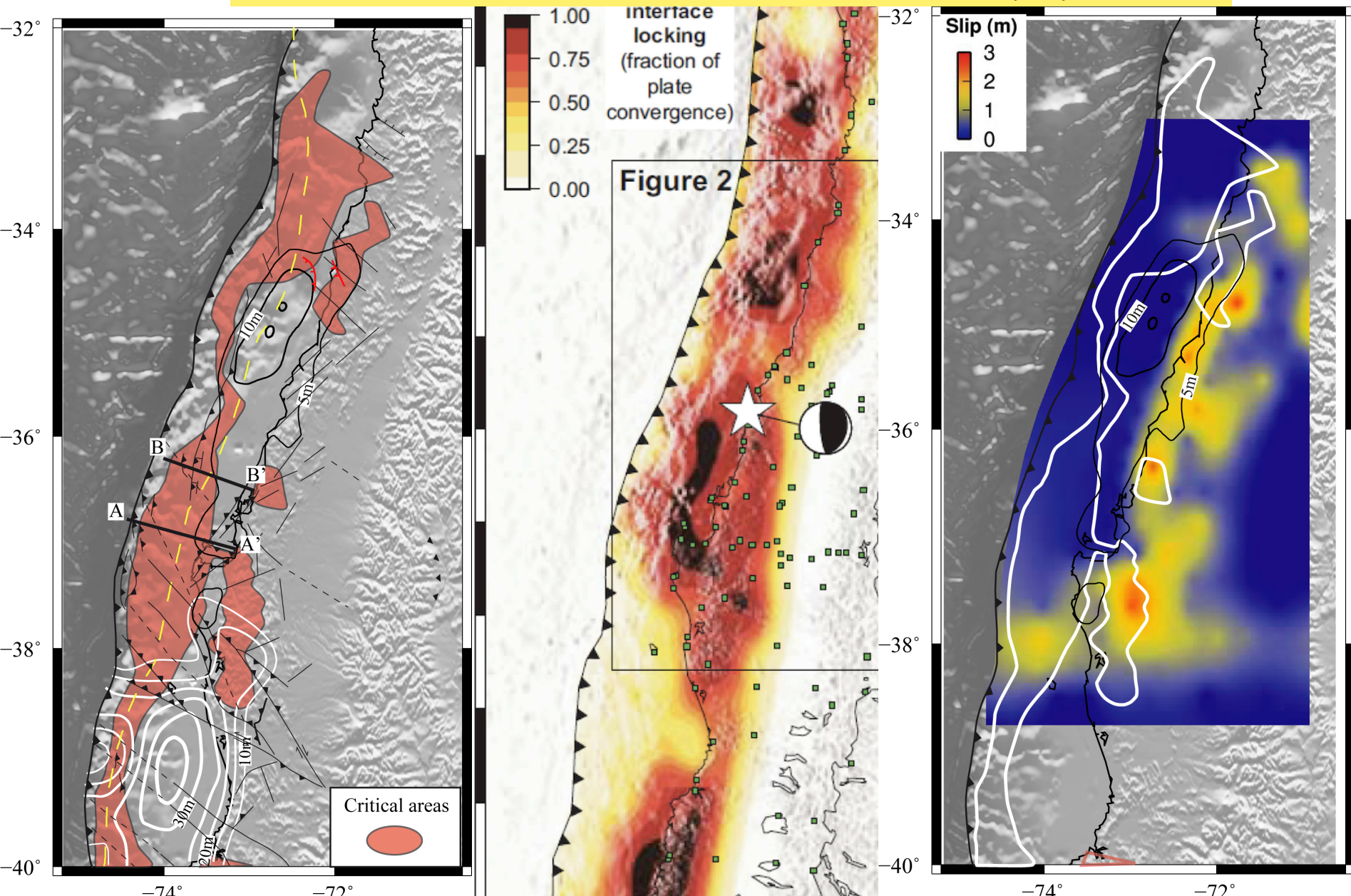
Comparison with coseismic slip (*Lin et al., JGR in prep.*)



*Moreno et al.,
GRL 2009*

2. Critical Taper

Comparison with interseismic (Moreno et al., *Nature* 2010, and postseismic slip (Lin et al., *JGR* in prep.)



Megathrust friction in the 2010 Maule earthquake area

1. Introduction

2. From the Critical Taper Theory

3. From Limit Analysis

4. From Dynamic Simulation of EQ cycle

3. Limit analysis

Theory (Salençon, 1974, 2002)

Based on:

➤ Force equilibrium: Theorem of virtual work

$$\mathcal{P}_i(\hat{\mathbf{U}}) = \mathcal{P}_e(\hat{\mathbf{U}}) \quad \forall \hat{\mathbf{U}} \text{ KA}$$

$$\mathcal{P}_e(\hat{\mathbf{U}}) = - \int_{\Omega} \overset{\text{Gravity term:}}{\rho g \mathbf{e}_2} \cdot \hat{\mathbf{U}} dV + \overset{\text{Pushing force:}}{Q \mathbf{t}_D} \cdot \hat{\mathbf{U}}_S$$

$$\mathcal{P}_i(\hat{\mathbf{U}}) = \int_{\Sigma_U} \overset{\text{Stress vector:}}{\hat{\mathbf{J}}} \cdot \mathbf{T} dS$$

➤ Theory of maximum rock strength (*Maillot and Leroy, 2006*)

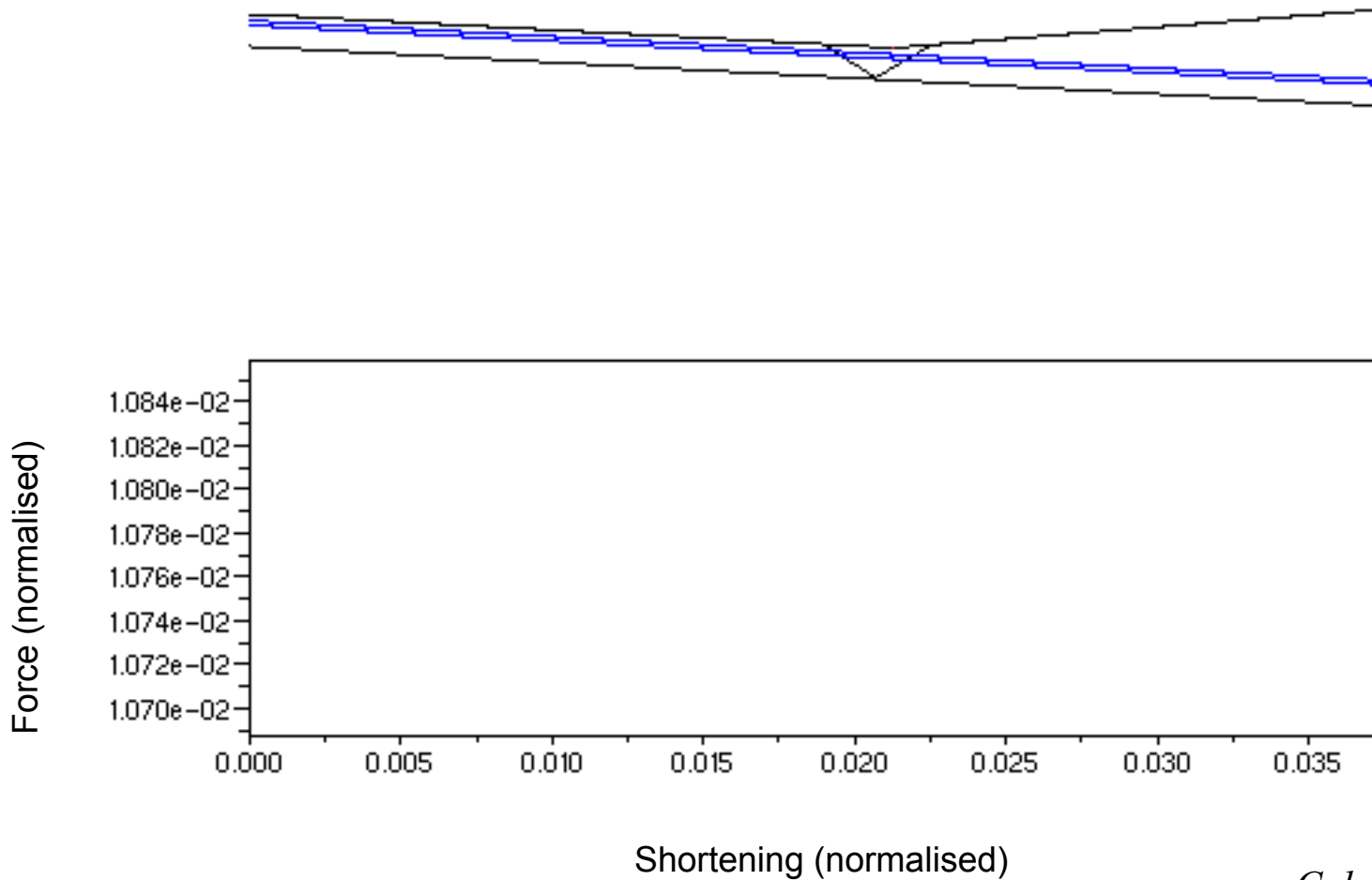
$$Q \mathbf{t}_D \cdot \hat{\mathbf{U}}_S \leq \int_{\Omega} \rho g \mathbf{e}_2 \cdot \hat{\mathbf{U}} dV + \int_{\Sigma_U} \varpi(\hat{\mathbf{J}}) dS$$

3. Limit analysis

Limit analysis

Based on:

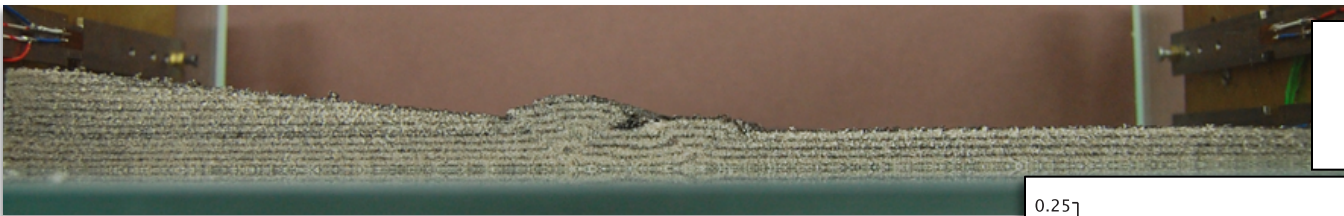
- Force equilibrium
- Theory of maximum rock strength



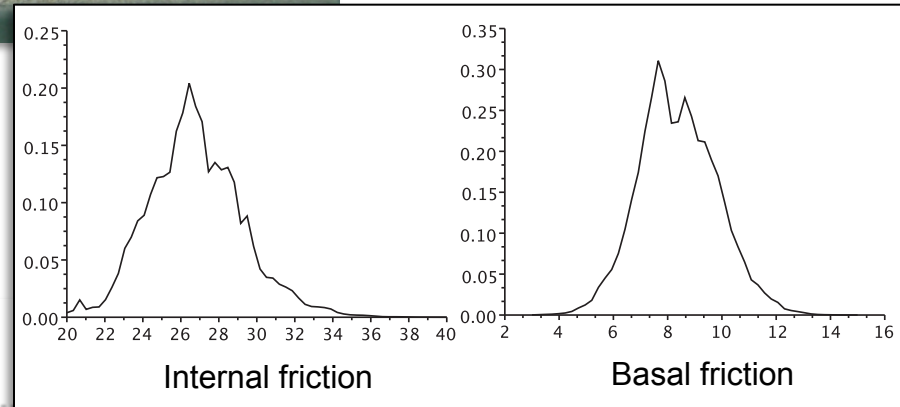
3. Limit analysis

Validation

Analogue experiments:



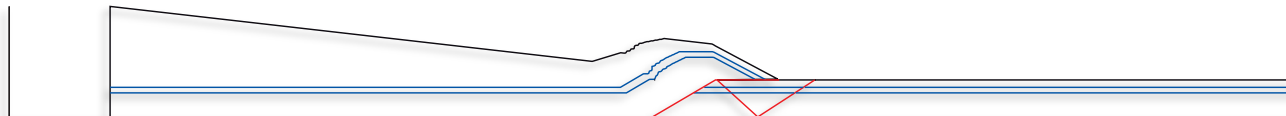
*Probability distributions
of frictional properties*



Statistical analysis: observable error bars



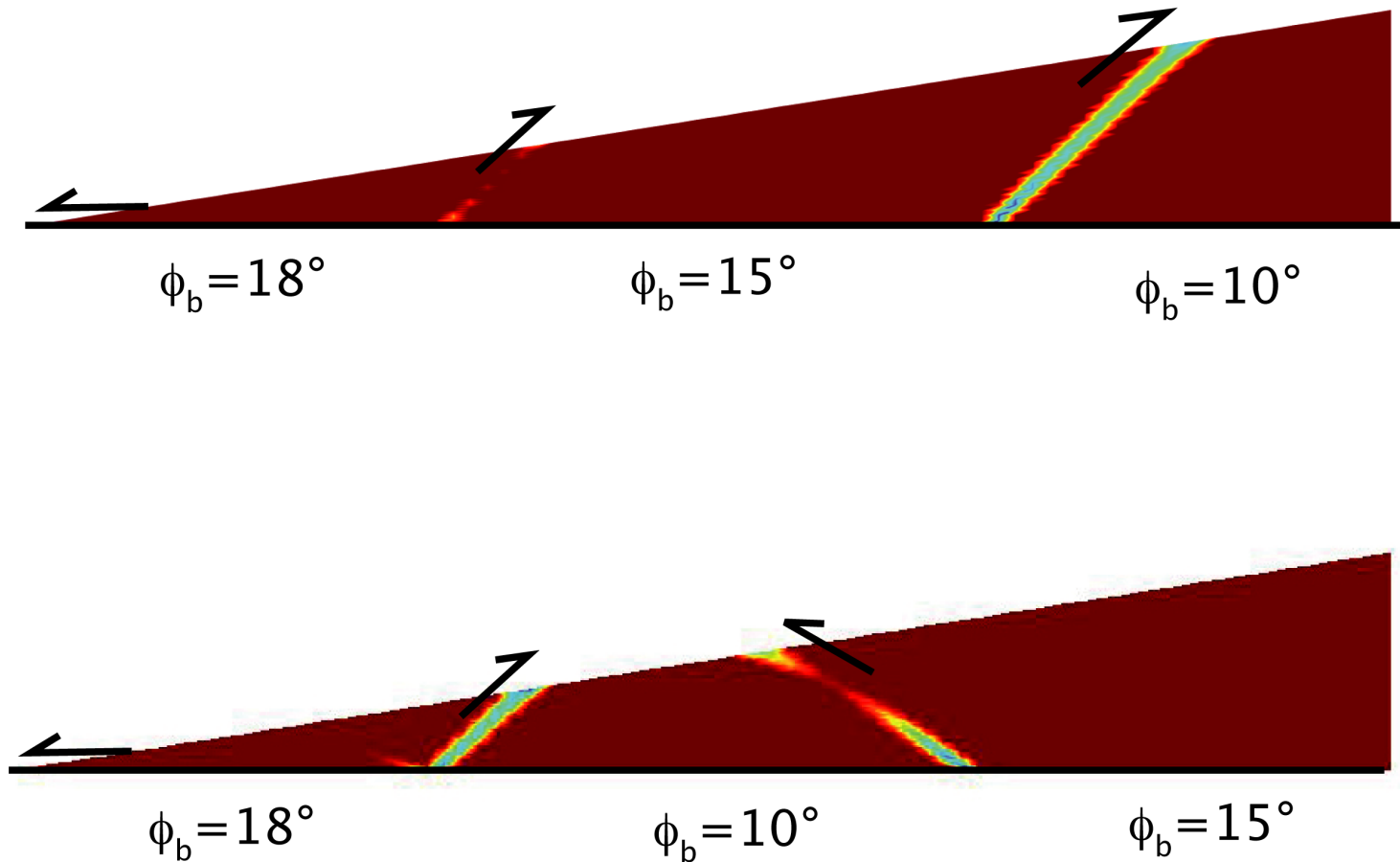
Mechanical modelisation:



3. Limit analysis

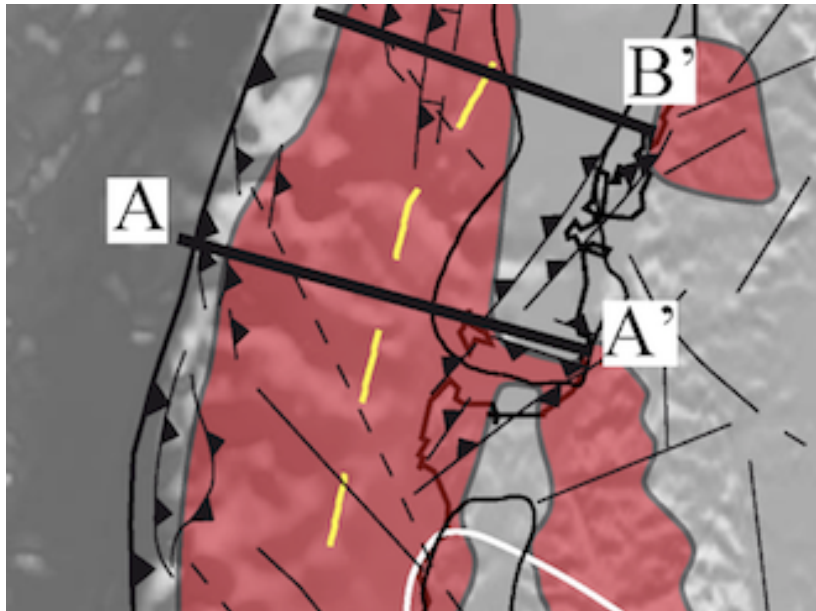
Active deformation: Transition of friction

Numerical limit analysis model: Souloumiac et al., Comp Geosc. 2010



3. Limit analysis

Active deformation: Transition of friction?



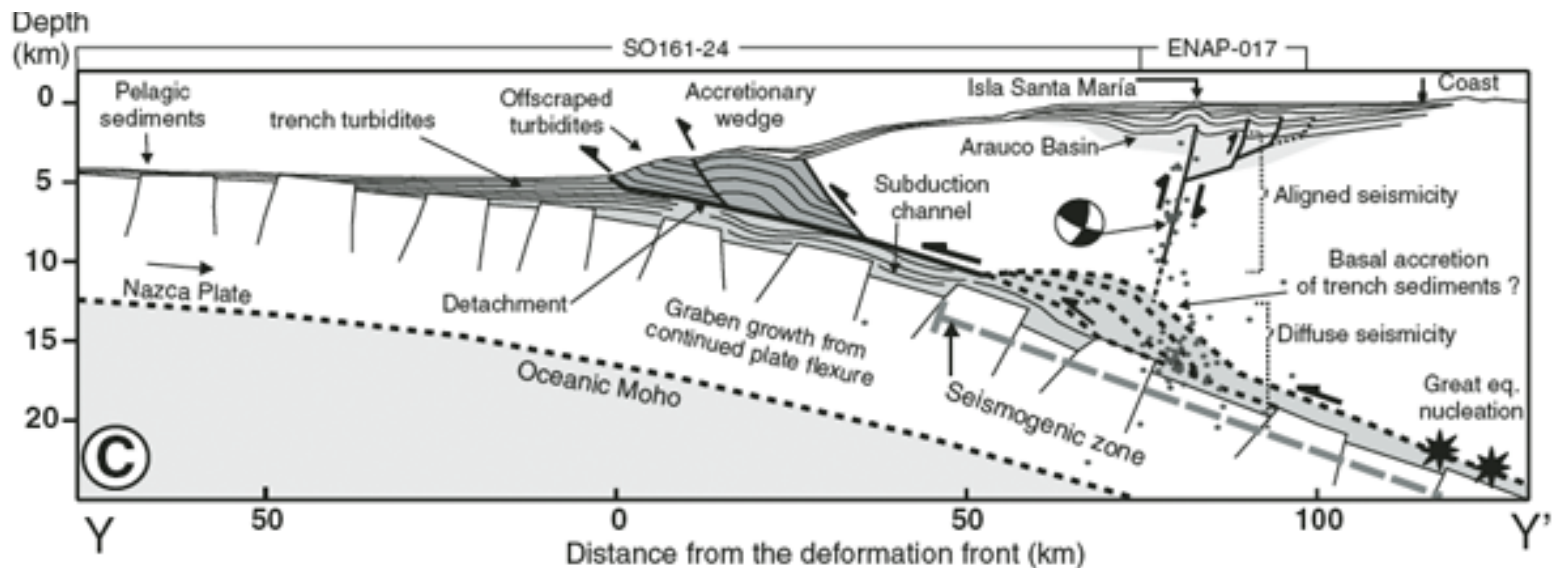
Isla Santa Maria:

2010 EQ : 1.4m uplift (Melnick et al., 2012)

1835 EQ : 2.4 - 3m (Darwin, 1839)

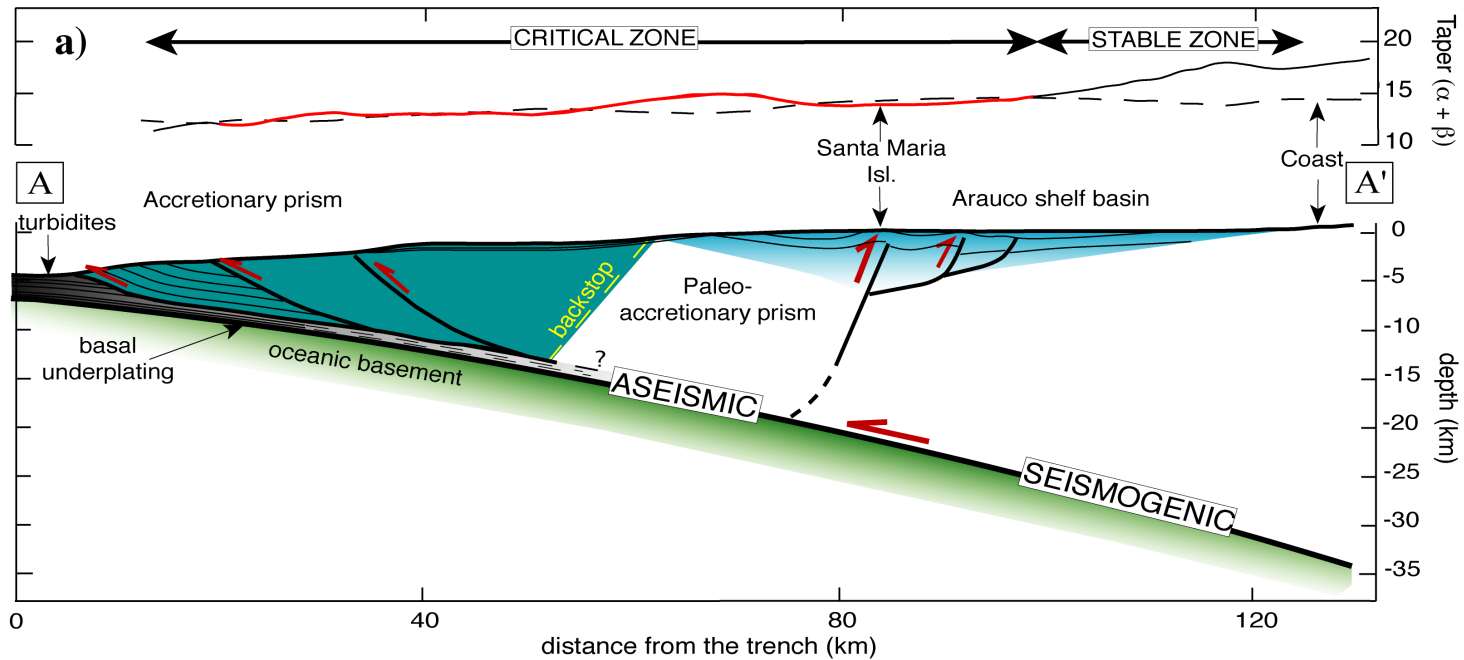
1751 EQ : 6m estimated (Melnick et al., 2006)

Long-term : 2m/ka since Pleistocene (Melnick et al., 2009)



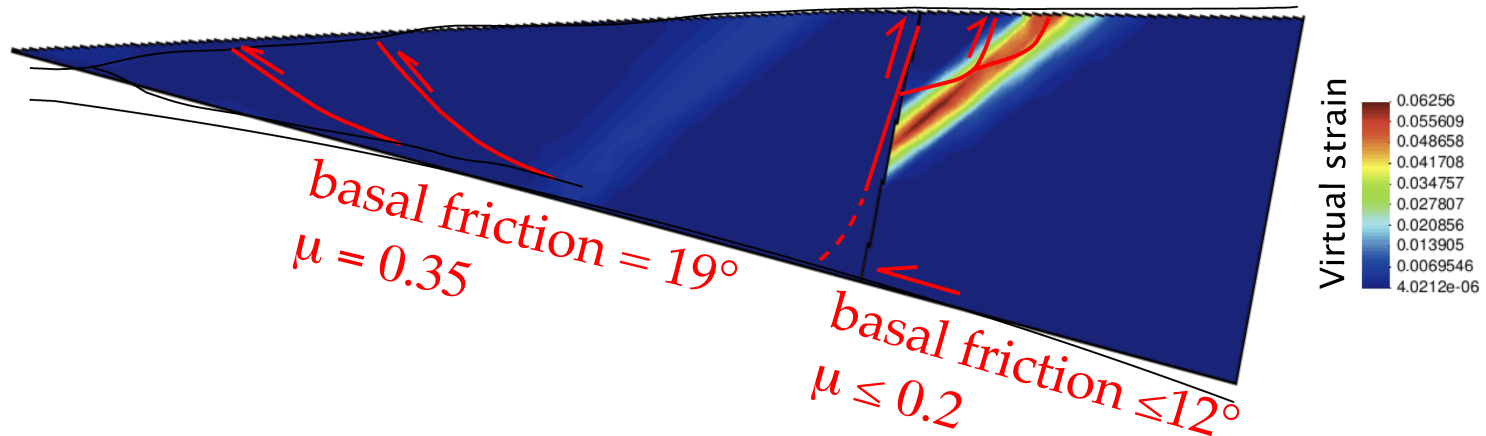
3. Limit analysis

Application to Santa Maria Island



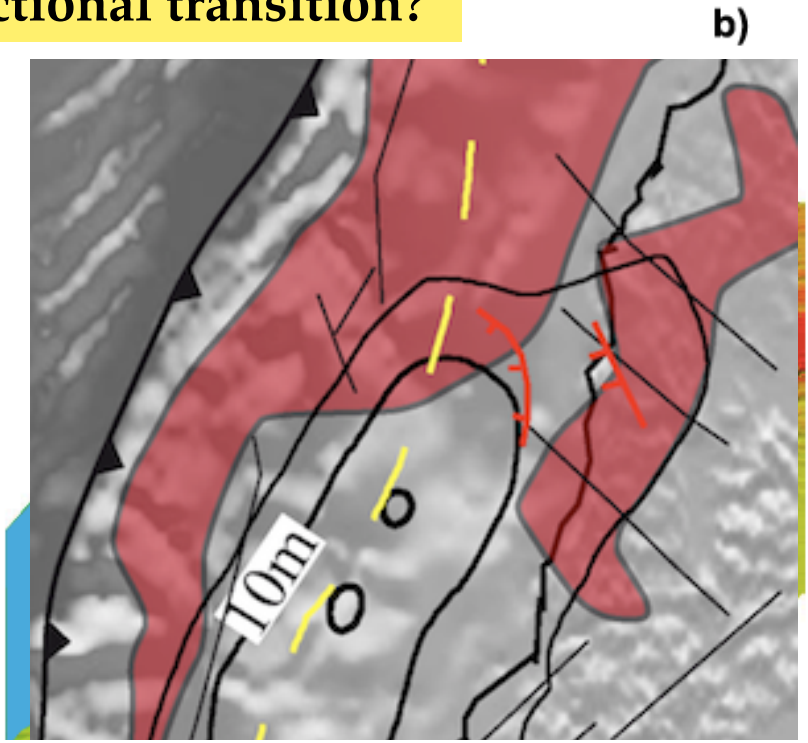
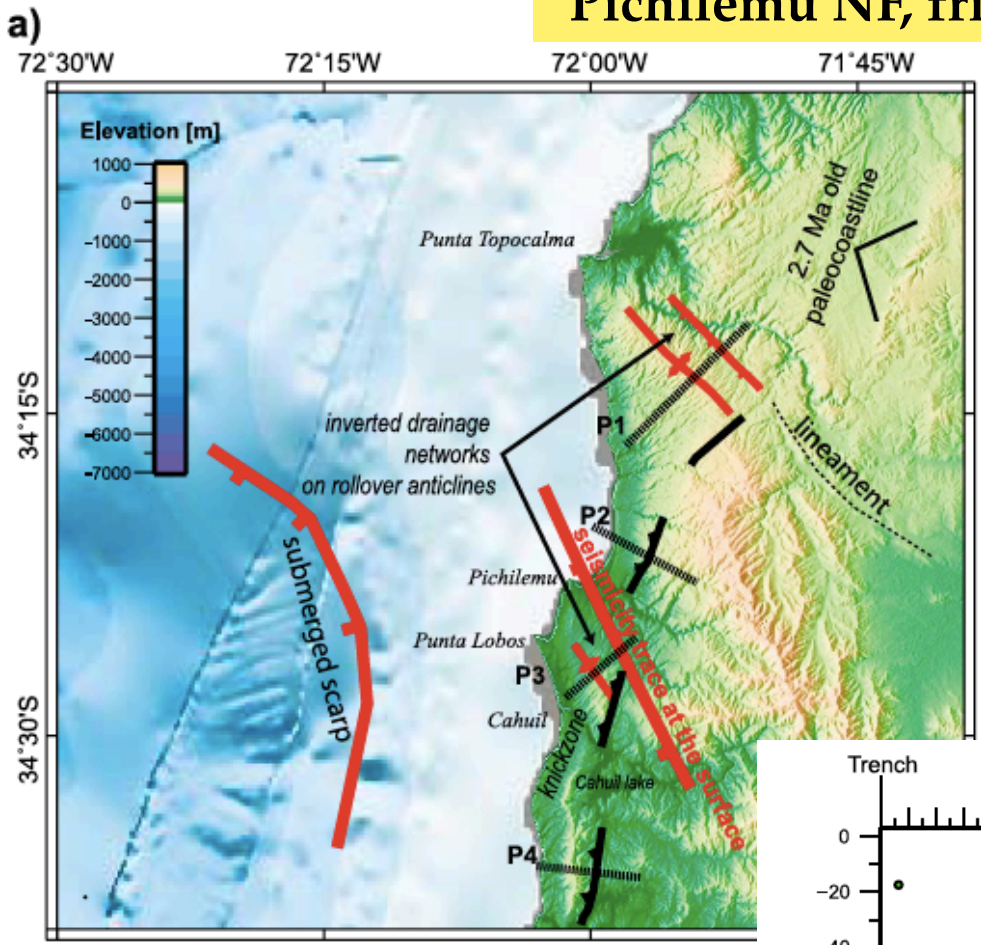
b)

Ramp friction = 12° , $\mu = 0.2$



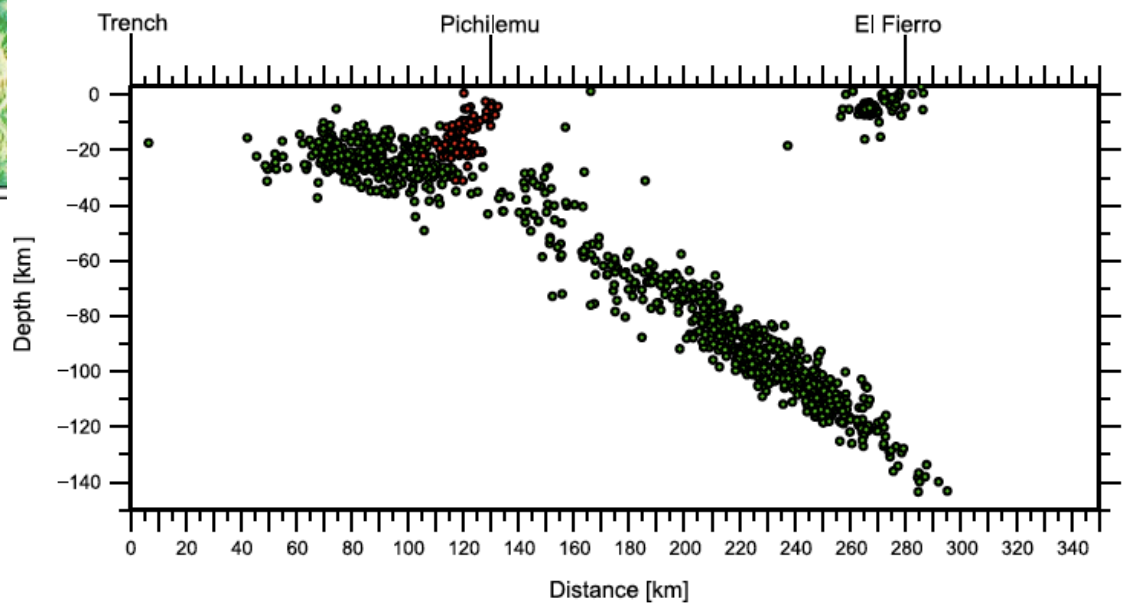
3. Limit analysis

Pichilemu NF, frictional transition?



Farias et al., Tectonics 2011

basal friction in SZ $\leq 5^\circ$
 $\mu \leq 0.1$

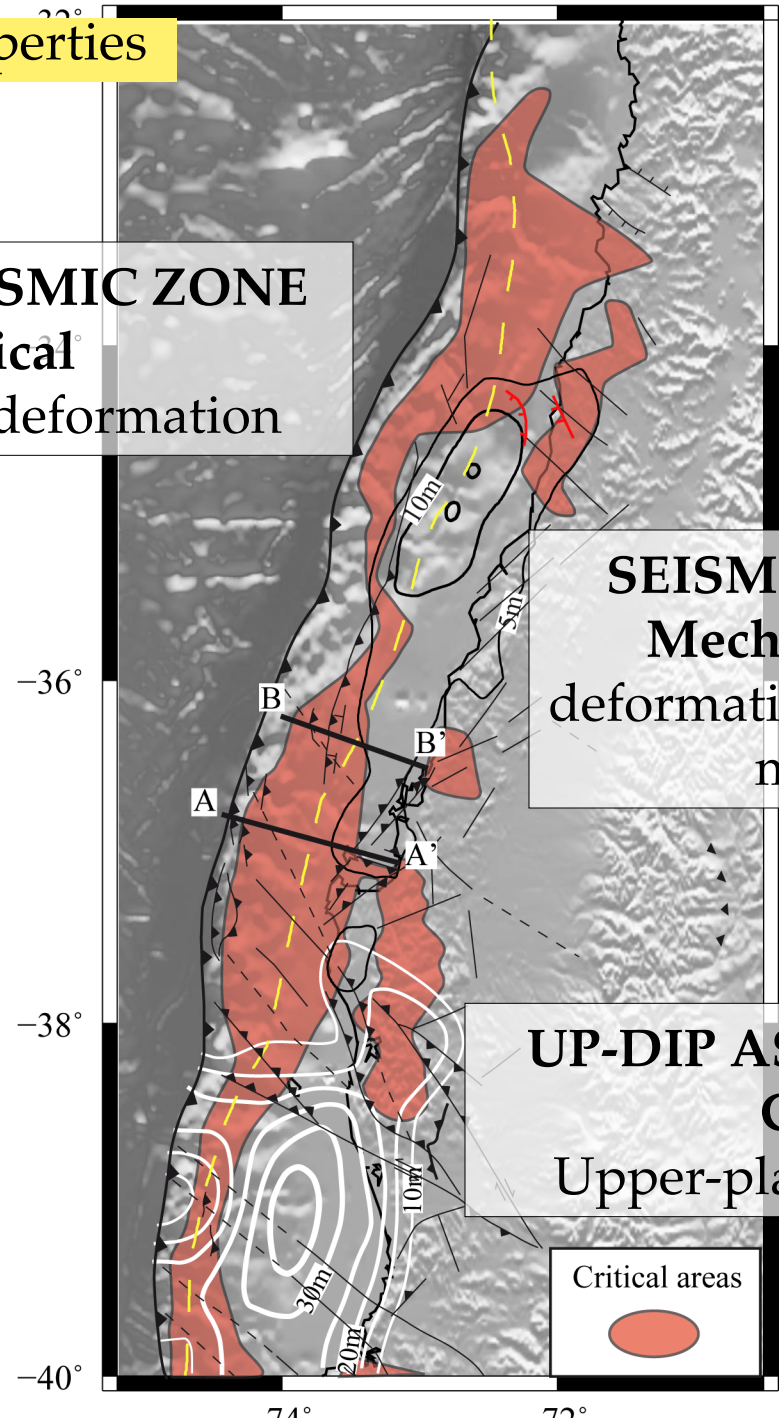



Forearc: Frictional properties

UP-DIP ASEISMIC ZONE
Critical
Upper-plate deformation

SEISMOGENIC ZONE
Mechanically stable
deformation localized on the
megathrust

UP-DIP ASEISMIC ZONE
Critical
Upper-plate deformation



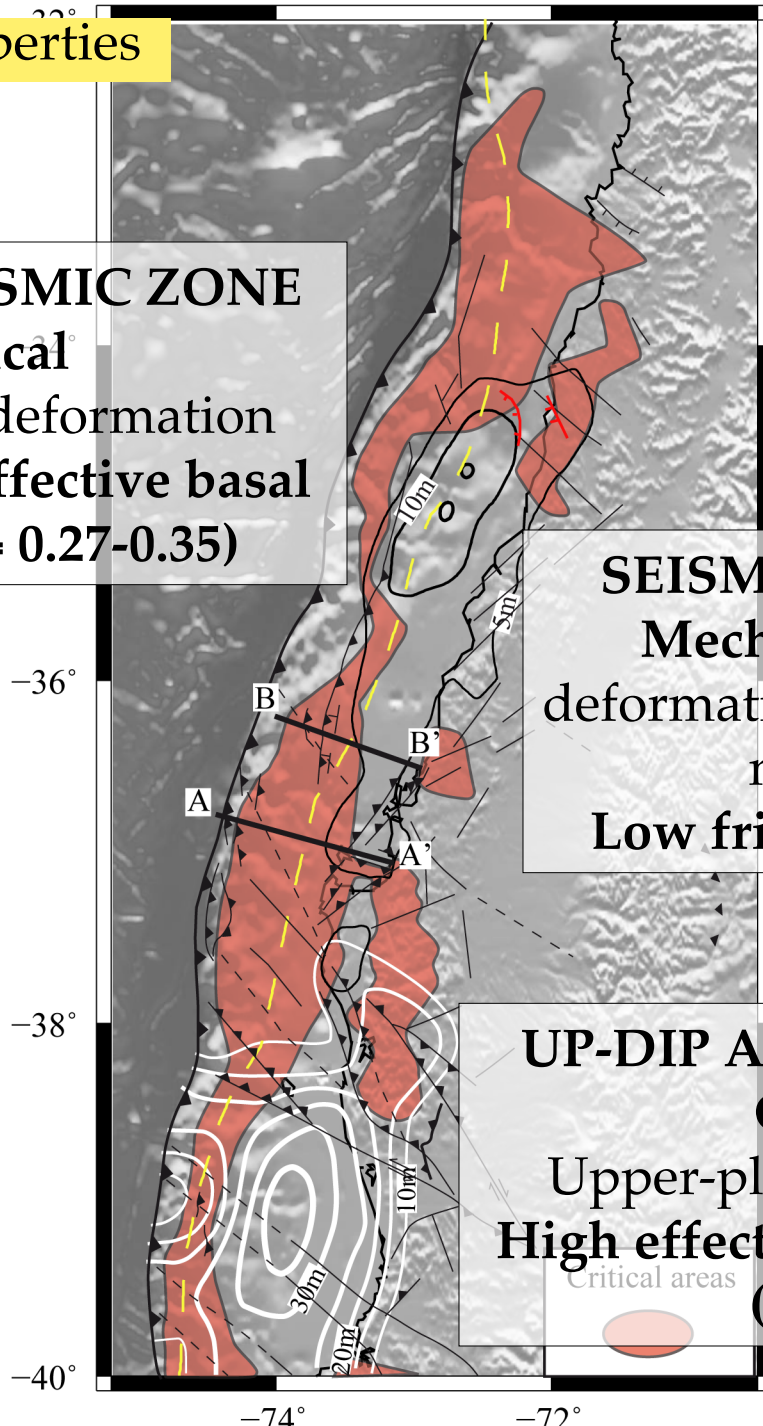
Critical areas


Forearc: Frictional properties

UP-DIP ASEISMIC ZONE
Critical
Upper-plate deformation
Intermediate effective basal friction ($\mu = 0.27-0.35$)

SEISMOGENIC ZONE
Mechanically stable
deformation localized on the
megathrust
Low friction ($\mu = 0.1-0.2$)

UP-DIP ASEISMIC ZONE
Critical
Upper-plate deformation
High effective basal friction ($\mu \geq 0.4$)



Forearc: Arauco Peninsula, a rate-strengthening barrier?

3D dynamic simulation of EQ cycle
(Lapusta and Liu, JGR 2009)

Based on Rate- and State- laws, laboratory-derived

(Dieterich, Ruina, Blanpied, Marone, Tullis and others, based on earlier work of Scholz and others) for slip velocities **small** ($\sim 10^{-9} - 10^{-2}$ m/s) compared to the seismic range.

Unique tool for simulating earthquake cycles in their entirety,

- from accelerating slip in slowly expanding nucleation zones
- to dynamic rupture propagation (*turn into linear slip weakening*)
- to post-seismic slip and interseismic creep
- to fault restrengthening between seismic events.

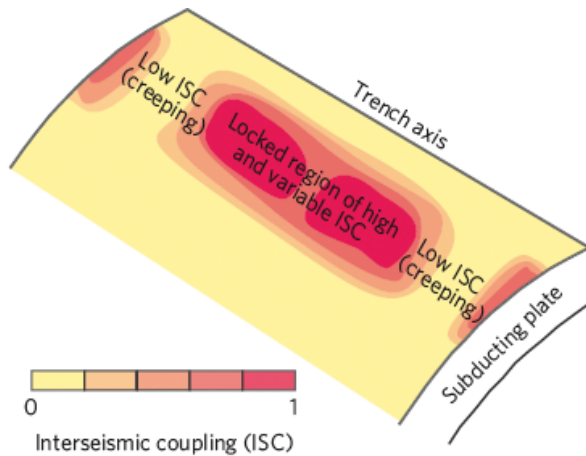
$$\tau = \bar{\sigma} f = (\sigma - p) \left[f_o + a \ln \frac{V}{V_o} + b \ln \frac{V_o \theta}{L} \right]; \quad \frac{d\theta}{dt} = 1 - \frac{V\theta}{L}$$

Forearc: Arauco Peninsula, a rate-strengthening barrier?

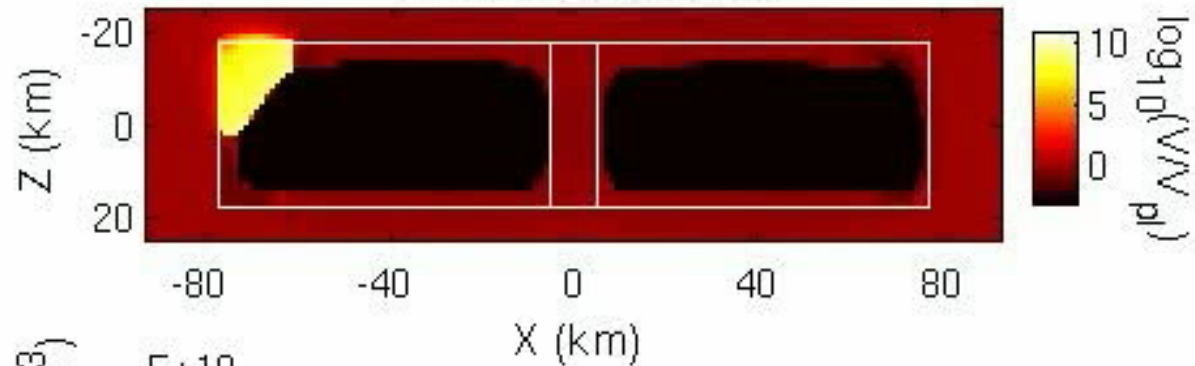
3D dynamic simulation of EQ cycle

Kaneko et al., Nature 2010

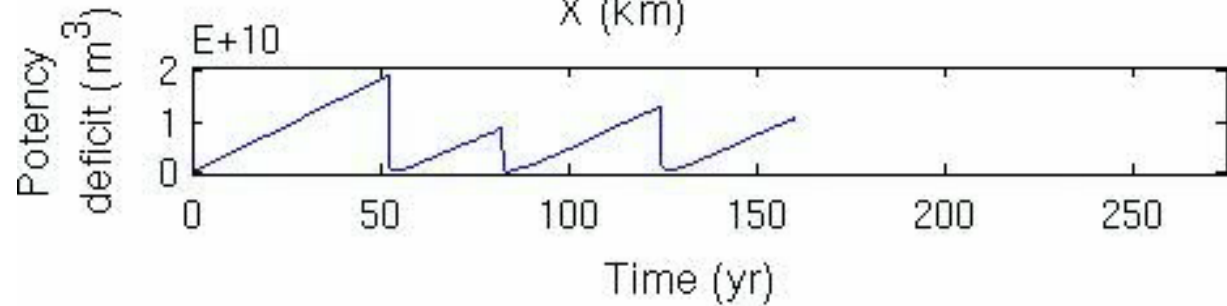
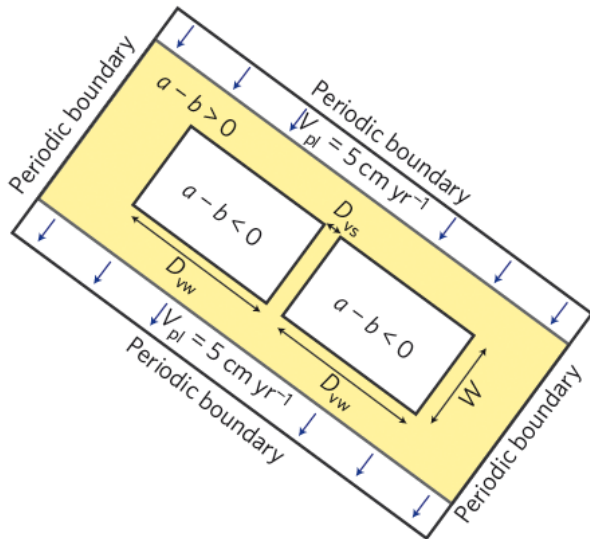
a



$t = 159.626021744 \text{ yr}$



c



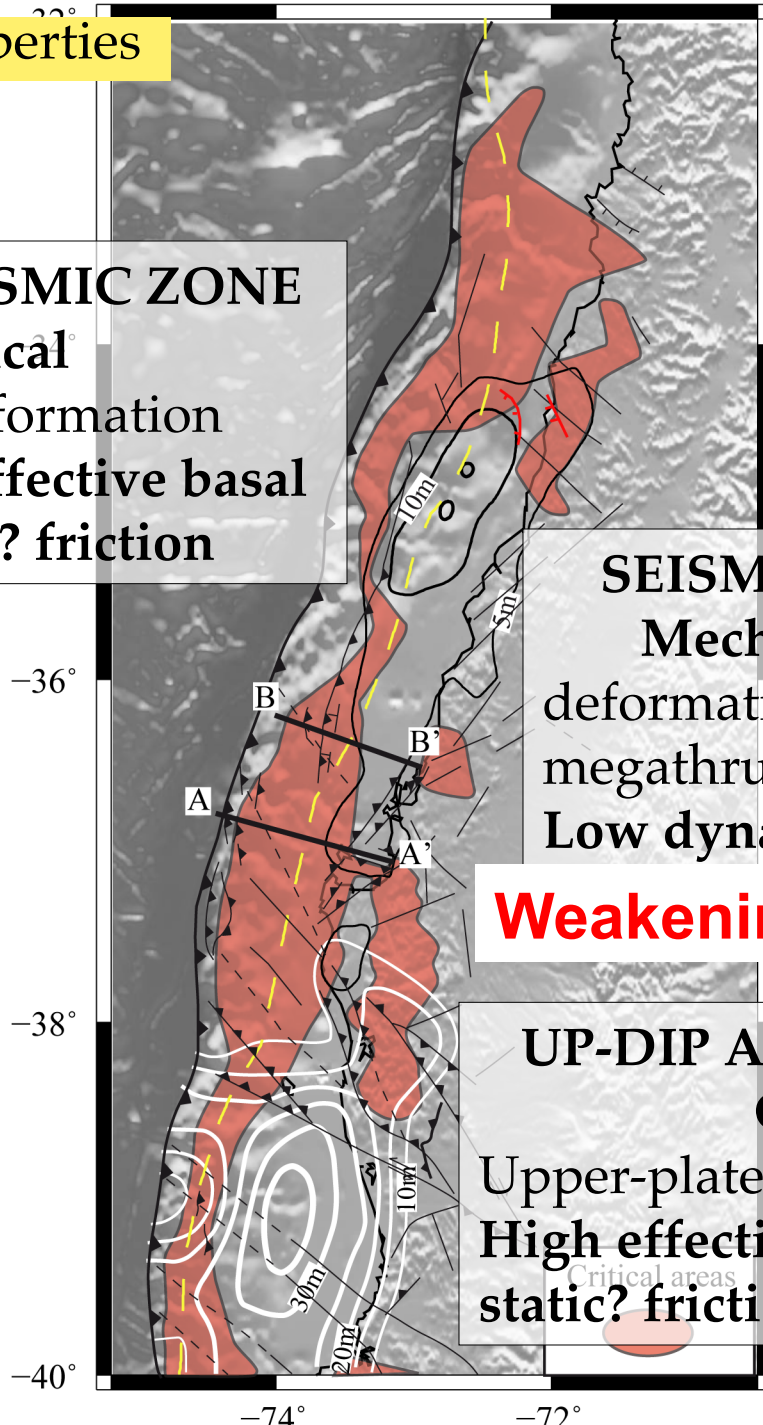
Forearc: Frictional properties

UP-DIP ASEISMIC ZONE
Critical
Upper-plate deformation
Intermediate effective basal friction = static? friction

SEISMOGENIC ZONE
Mechanically stable
deformation localized on the megathrust
Low dynamic? friction

Weakening mechanism?

UP-DIP ASEISMIC ZONE
Critical
Upper-plate deformation
High effective basal friction = static? friction



Megathrust friction in the 2010 Maule earthquake area

1. Introduction
2. From the Critical Taper Theory
3. From Limit Analysis
4. From Dynamic Simulation of EQ cycle

4. 2-3D Dynamic simulation

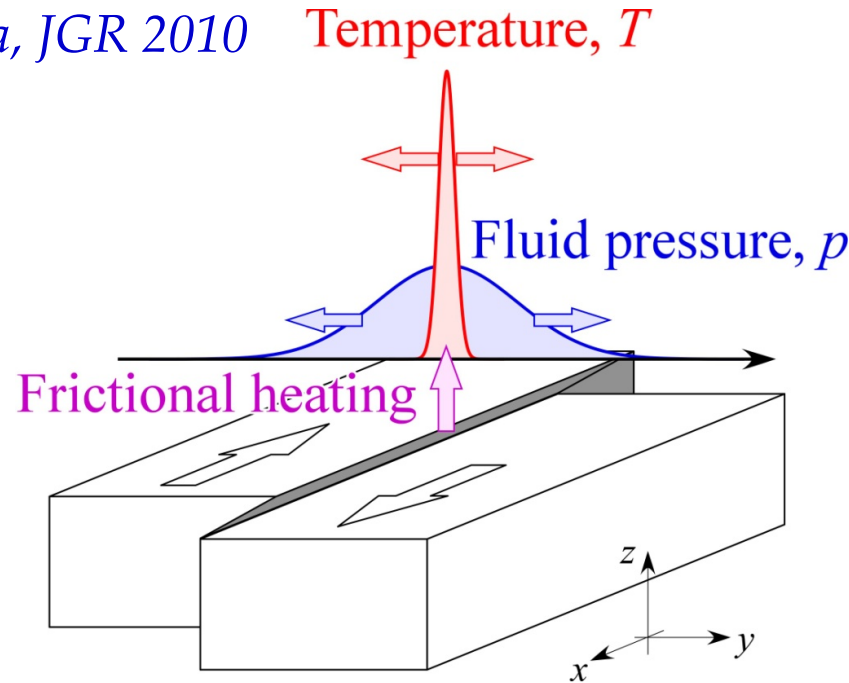
Weakening mechanisms

Hydrothermal effects on frictional resistance (high slip rates)

(Sibson 1973, Lachenbruch 1980, Mase & Smith 1985, Lee & Delaney 1987, Andrews 2002, Wibberley 2002, Noda & Shimamoto 2005, Sulem 2005, Bizarri & Cocco 2006, Rice 2006,...)

Numerical implementation: *Noda and Lapusta, JGR 2010*

- Rapid shear heating during seismic slip increases fault temperature T .
- **Thermal pressurization** is one of the potential effects: Since the thermal expansivity of water is much larger than that of rocks, shear heating may increase the pore fluid pressure p .
- This could lead to **co-seismic fault weakening**, additional to any slow-slip friction behavior.



$$\text{Shear traction } \tau = f \sigma_e = f (\sigma_n - p) \text{ --- Pore pressure}$$

Friction coefficient Effective normal stress Elastodynamic normal stress

4. 2-3D Dynamic simulation

Model set-up

Important *length scales* to resolve:

Nucleation size:

Seismic slip in large enough regions -
Estimates of the critical size (Rice and
Ruina, 1983; Rice, Lapusta, Ranjith, 2001;
Rubin and Ampuero, 2005):

$$h^* \propto \frac{\text{shear modulus} \times \text{char. slip}}{\text{effective normal stress} \times F(a, b)}$$

$$h_{RR}^* \propto \frac{\mu L}{\bar{\sigma}(b-a)}; \quad h_{RA}^* \propto \frac{\mu L}{\bar{\sigma}(b-a)^2 / b}$$

Characteristic weakening scale at the rupture tip due to RS friction

$$\Lambda = \frac{\mu^* L}{b\sigma}$$

Important *slip scales* to resolve:

For adiabatic, undrained conditions (Rice 2006):

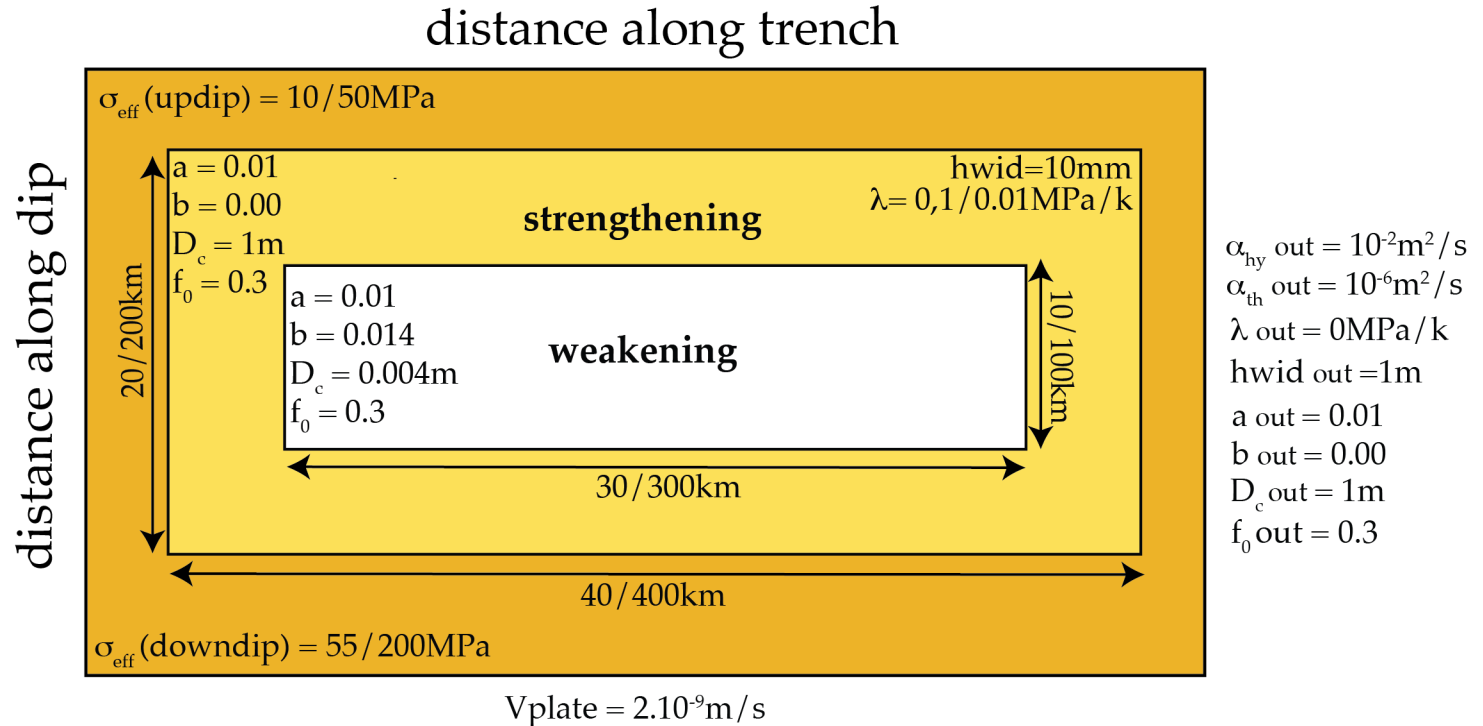
$$La = \frac{\text{specific heat} * \text{layer thickness}}{\text{friction} * \text{undrained press factor}}$$

At constant friction & slip rate (Rice 2006):

$$L^* = \frac{4}{f^2} \left(\frac{\rho c}{\Lambda} \right)^2 \frac{\left(\sqrt{\alpha_{hy}} + \sqrt{\alpha_{th}} \right)^2}{V}$$

4. 2-3D Dynamic simulation

Model set-up

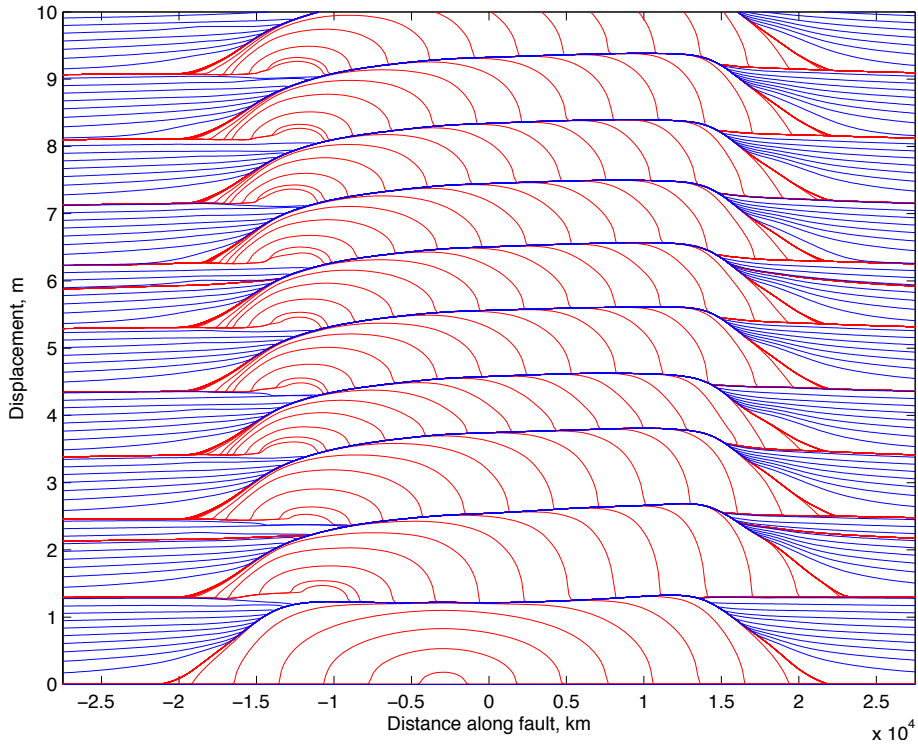


- $f_0 = 0.6$ - no TP
- $f_0 = 0.3$ - no TP
- $f_0 = 0.6$ - TP: $\alpha_{\text{hy}} = 10^{-3}\text{m}^2/\text{s}$
- $f_0 = 0.6$ - TP: $\alpha_{\text{hy}} = 10^{-4}\text{m}^2/\text{s}$

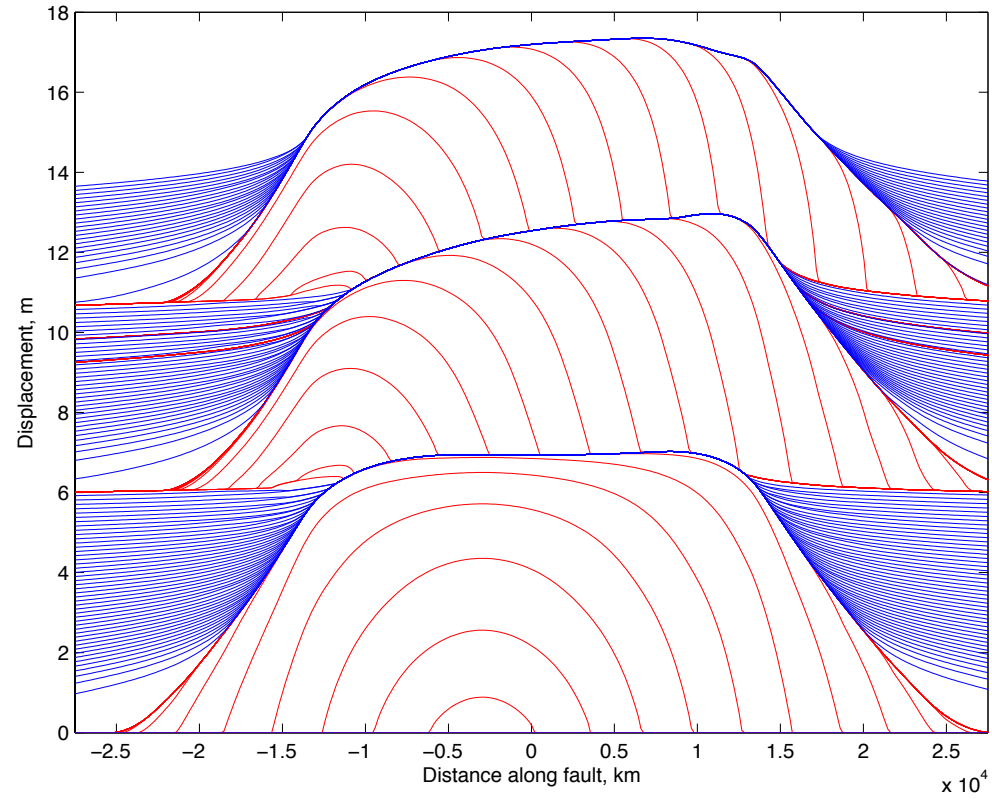
4. 2-3D Dynamic simulation

Dynamic friction, stress drop and recurrence

no TP

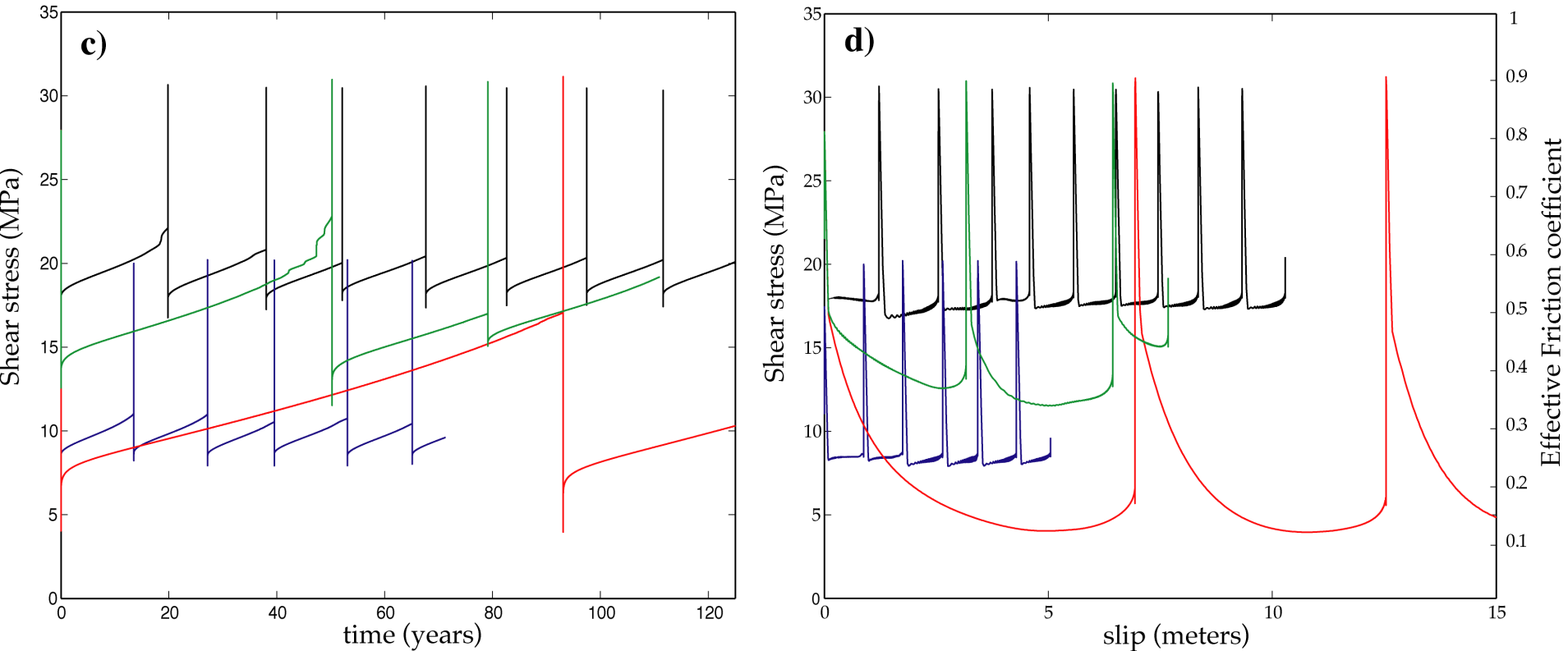


with TP



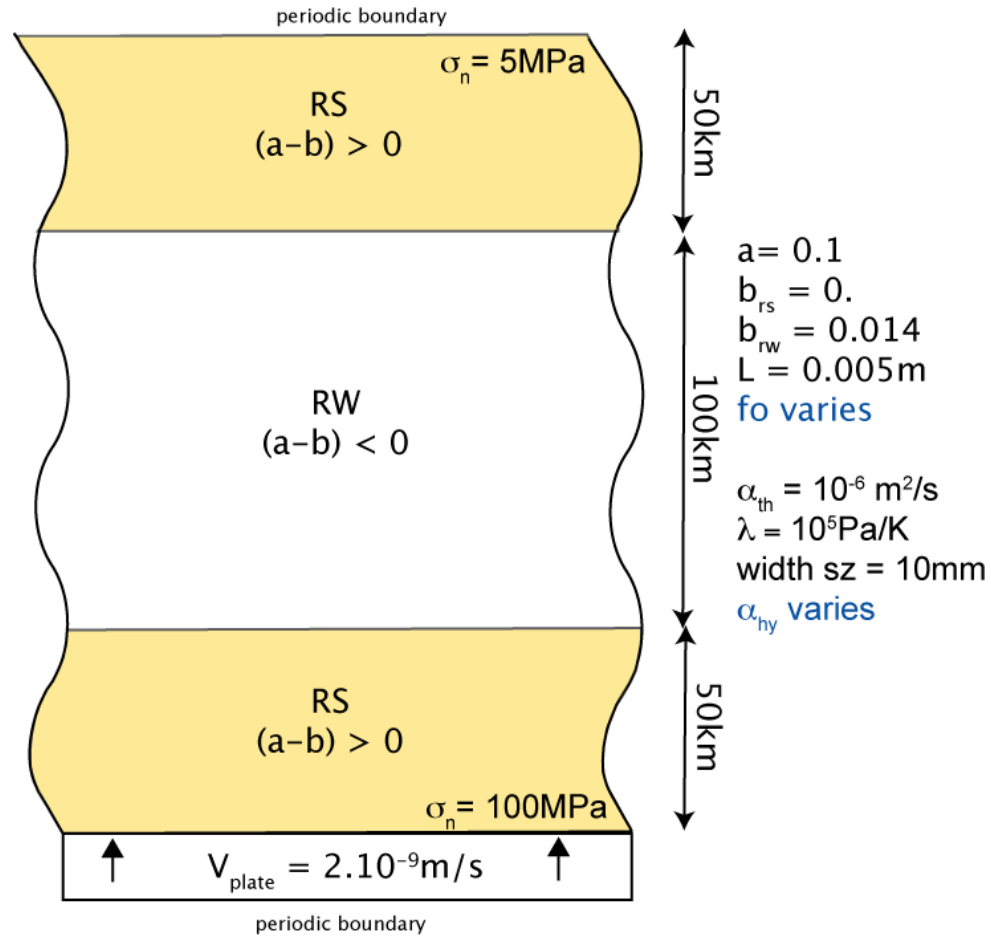
4. 2-3D Dynamic simulation

Dynamic friction, stress drop and recurrence



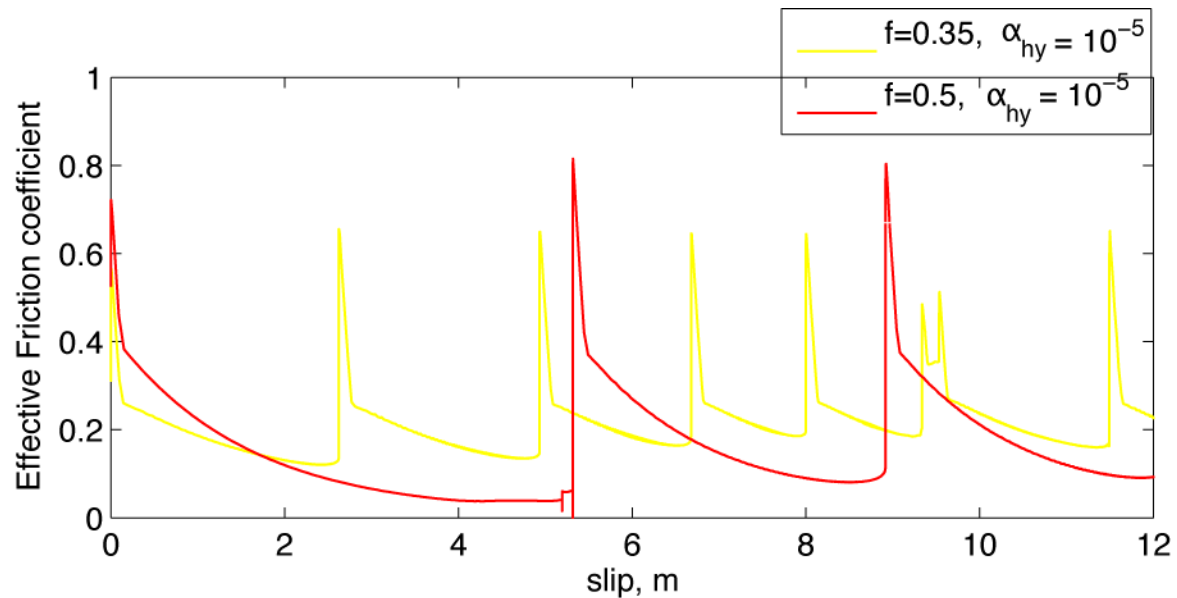
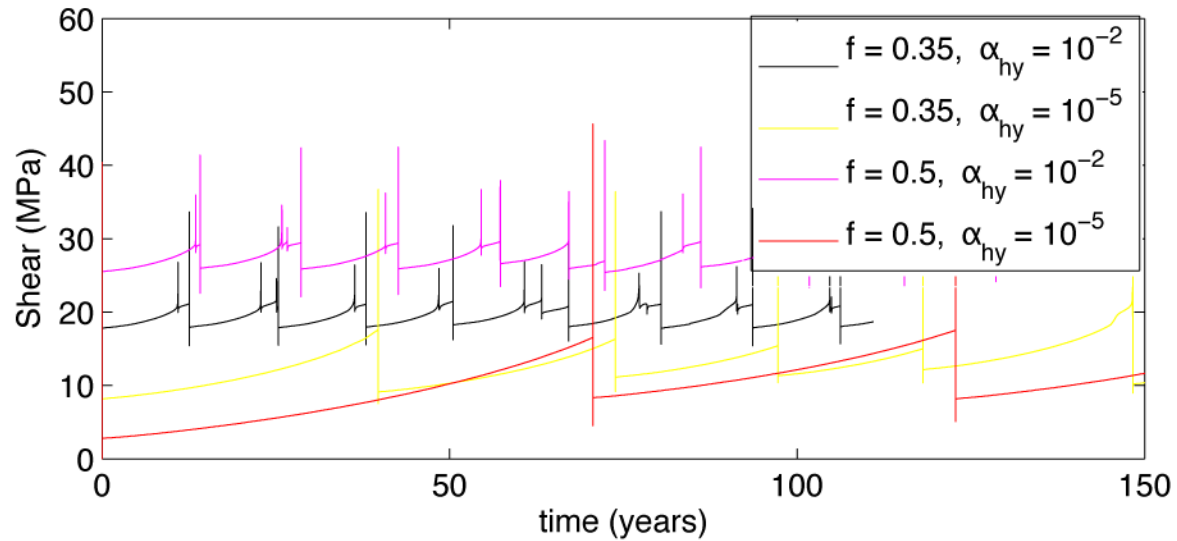
4. 2-3D Dynamic simulation

Model set-up



4. 2-3D Dynamic simulation

Dynamic friction, stress drop and recurrence



Conclusion

